Regular Article

PHYSICAL CHEMISTRY RESEARCH
Published by the
Iranian Chemical Society
www.physchemres.org
info@physchemres.org

Phys. Chem. Res., Vol. 11, No. 4, 801-823, December 2023
DOI: 10.22036/pcr.2022.359603.2177

Computational Investigation of Geniposidic Acid as an Anticancer Agent Using Molecular Docking, Molecular Dynamic Simulation, DFT Calculation, and OSIRIS-Molinspiration Profiling

B.C. Joshi[a], V. Juyal[a], A.N. Sah[a] and S. Saha[b,*]

[a]*Department of Pharmaceutical Sciences, Faculty of Technology, Sir J.C. Bose Technical Campus, Bhimtal, Kumaun University, Nainital-263136, Uttarakhand, India*

[b]*School of Pharmaceutical Sciences & Technology, Sardar Bhagwan Singh University, Dehradun, 248161 Uttarakhand, India*

(Received 29 August 2022, Accepted 12 November 2022)

Geniposidic acid is an iridoid glycoside. Iridoid glycosides showed antitumor, anti-inflammatory, cardiovascular, anti-hepatotoxic, choleretic, hypoglycaemic, hypolipidemic, antispasmodic, antiviral, immunomodulatory, and purgative activities. In this study, we focused on an iridoid glycoside geniposidic acid and computationally established the molecule as an anticancer drug. By doing so, we performed molecular docking, molecular dynamic simulation, DFT calculation, and OSIRIS-MOLINSPIRATION profiling targeting various oncogenic receptors. Outcomes suggested that geniposidic acid showed good interactions with 4DRH, 4AG8, and 4HJO. As these receptors showed anticancer activity by interacting with peptidylprolyl isomerase, VEGFR2, and EGFR tyrosine kinase**,** it might be possible that geniposidic shows its activity in the same way. RMSD, RMSF, R_g, and SASA values of docked conformers create a positive impact on receptor interaction. DFT (Density functional theory) calculation stated that HOMO (Highest Occupied Molecular Orbital) orbital of geniposidic acid mainly delocalized on the total aglycone part, and in the case of LUMO (Lowest Unoccupied Molecular Orbital) orbital image showed that the total electron cloud focused on C-O-C=C-COOH group of aglycone part. In-silico profiling of geniposidic acid showed that the molecule positively interacted with G-protein coupled receptor (GPCR) and nuclear receptors. This information collectively confirms that if we relaunch geniposidic acid in a pharmacologically established manner, then it will be a boon for mankind to treat cancer.

Keywords: Geniposidic acid, Molecular docking, MD simulation, DFT calculation, OSIRIS-MOLINSPIRATION

INTRODUCTION

Cancer is described as the unregulated growth of cells caused by the dysregulation of cell signaling pathways and the dispersion of invasive neoplastic cells in various tissues, making cancer a multifactorial disease [1-2]. Cancer is a global health challenge because of its high occurrence worldwide, it claims about 8 million deaths per year with 14 million new cases annually [3]. Cancer initiation, propagation, and progression are three distinguishable phases of carcinogenesis [4]. Multiple mutations disrupt signaling pathways, which have been linked to cancer development [5,6]. The MAPK (Mitogen-Activated Protein Kinase) signaling cascade [7,8] plays an important role in tumor progression, oncogenesis [9], and drug resistance [10-12]. The ErbB/HER (Erythroblastic Oncogene-B/Human Epidermal growth factor receptor) family plays a decisive role in the proliferation, differentiation, migration, and survival of cells [13,14]. EGFR mutations and overexpression have been linked to the occurrence and spread of several cancers, most notably breast, lung, prostate, bladder, ovary, and pancreatic cancers [15,16]. At the molecular level, stimulation of EGFR (Epidermal growth factor receptor) induces intrinsic tyrosine kinase activity and cellular signaling those results in cell growth and proliferation [17-18]. As a result, 99% of EGFR tyrosine

*Corresponding author. E-mail: supriyo9@gmail.com

kinase inhibitors, such as Iressah (gefitinib) and Tarcevah (erlotinib) [19-22], are highly effective against lung cancers; Zactimah (Vandetanib) is highly effective against late-stage medullary thyroid cancer, and Tykerbh (Lapatinib) is highly effective against metastatic breast cancer [23-27]. In connection with the development of anticancer agents, various synthetic molecules were developed, but synthetic molecules were associated with huge side effects [28-30]. In this context, anticancer agents isolated from natural sources were observed with greater efficacy and fewer side effects. In terms of this connection, our research focused on Premna barbata Wall. ex Schauer (Family: Lamiaceae) [31,32]. Many active phytoconstituents are reported in this plant, including iridoid glycosides, flavonoids, and terpenoids [33-35]. Among other iridoid glycosides, geniposidic acid is the main constituent obtained from *Premna barbata*. Geniposidic acid was also isolated from *Avicennia officinalis, Gardenia jasminoides, Premna barbata,* and *Premna integrifolia* [36,37] (Fig. 1). Till now, the antitumor activity of geniposidic acid has been reported [38]. The cause behind the partial exploration of geniposidic acid was the natural low abundance [39]. Earlier studies reported that iridoid glycosides were observed with antitumor, anti-inflammatory, cardiovascular, anti-hepatotoxic, choleretic, hypoglycaemic, hypolipidemic, antispasmodic, antiviral, immunomodulatory, and purgative activities [40]. Recently, reported that leaves of *Dipsacus fullonum* L showed good anticancer activities against breast cancer [41]. In this study, we performed molecular docking, molecular dynamic simulation, DFT calculation, and OSIRIS-MOLINSPIRATION profiling of geniposidic acid targeting various oncogenic targets.

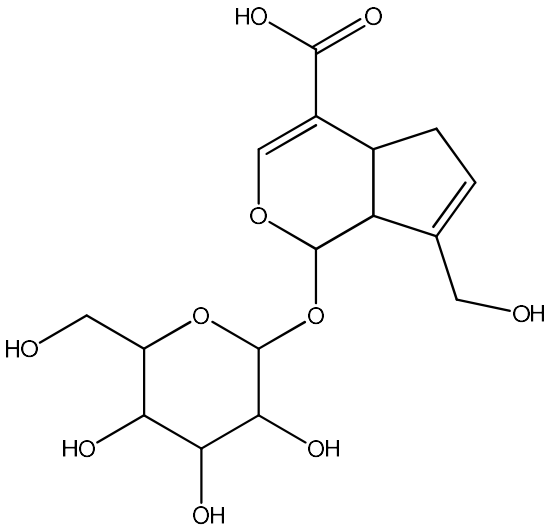

Fig. 1. Structure of geniposidic acid.

MATERIALS AND METHODS

Structural Information of Geniposidic Acid

The structure of geniposidic acid contained five hydrogen bond donors, ten hydrogen bond acceptors, one negative ion, and one hydrophobic group. The molecular formula, formula weight, molar refractivity, molar volume, parachor value, and surface tension of geniposidic acid are $C_{16}H_{22}O_{10}$, 374.3398, 83.74 cm^3, 226.9 cm^3, 702.1 cm^3, and 91.6 dyne/cm, respectively [42]. As geniposidic acid was partially explored in terms of applicability, there is a chance that geniposidic acid comes under pan assay interference compounds (PAINS) in high throughput screening, so we also checked that possibility. The detailed search showed that toxoflavin, isothiazolones, hydroxyphenyl hydrazones, curcumin, phenol-sulfonamides, rhodanines, enones, quinones, and catechols were observed as PAINS, [43] but after the development of the electronic filter, dicyanoalkene is an authorized PAINS. So, we easily confirmed that geniposidic acid in whole or in part does not belong to the PAINS category.

Molecular Docking Studies of Geniposidic Acid against Different Oncogenic Targets

In this way, we mainly focused on epidermal growth factor receptor (EGFR) kinase, tyrosine kinase, mitogen-activated protein kinase-1 (MAPK), estrogen receptor alpha, cyclic adenosine monophosphate dependent protein kinase, peptidylprolyl isomerase, progesterone receptor, forkhead box protein M1 DNA, caspase, human epidermal growth factor-2, cyclin-dependent kinase 2/cyclin-A complex, hepatitis C virus polymerase, and vascular endothelial growth factor receptor-2 binding protein receptors. There was an obvious question that arise in mind. Why do we select these oncogenic targets? EGFR activation up-regulates the PI3K/AKT cascade, which acts as a potent driver for tumor initiation and progression, leading to the inhibition of apoptosis, cellular proliferation, promotion of angiogenesis,

and metastasis [44]. Mutations in the ESR1 gene lead to abnormal MAPK signalling that may contribute to increased or uncontrolled cell proliferation along with resistance to apoptosis [45]. Overexpression of Ca^{2+}/cAMP signalling (a molecular timer of the cell cycle) is responsible for abnormal proliferative responses leading to cancer [46]. A high level of Pin1 is also responsible for higher proliferative capacity and downregulates tumour suppressors, PI3K-AKT, Ras-ERK, and the JNK/p38MAPK signalling cascade [47,48]. The caspase enzyme plays an important role in apoptosis [49]. Overexpression and amplification of HER-2 also lead to cancer progression [50]. CDKs (checkpoints) act as a surveillance system that detects abnormalities during cell cycle progression [51]. HCV enters the host, replicates in hepatocytes, and releases its protein component in the cytosol which leads to a variety of cellular and immune-mediated changes that lead to HCC [52]. Hypoxia and dysregulation of growth factors PDGF, EGF, IGF-1, and TGF-α, and mutation lead to overexpression of VEGF, causing cancer [53].

Epidermal Growth Factor Receptor Kinase: 1M17, 2J6M, 3QWQ, 4HJO, 3GOP, 4LQM, 4R3R, 4ZJV, and 5XWD (receptor PDB id) were Selected

1M17. 1M17 is an EGFR tyrosine kinase receptor complexed with erlotinib. The receptor was isolated from *Homo sapiens* with *Spodoptera frugiperda* as an expressing system. The receptor belongs to the transferase category with E.C number 2.7.1.112. It has one chain with 333 amino acids [54].

2J6M. 2J6M is an EGFR kinase receptor complex with AEE788. The receptor was isolated from Homo sapiens with Spodoptera frugiperda as an expressing system. The receptor belongs to the transferase category with E.C number 2.7.1.112. It has one chain with 327 amino acids [55].

3QWQ. 3QWQ is a crystal structure of the extracellular domain of the EGFR in a complex with an adnectin. The receptor was isolated from Homo sapiens with Escherichia coli and Spodoptera frugiperda as expression systems. The receptor belongs to the protein binding/signalling protein category with E.C number 2.7.10.1. It has one chain with 258 amino acids [56].

4HJO. 4HJO is a crystal structure of the inactive EGFR tyrosine kinase domain with erlotinib. The receptor was isolated from Homo sapiens with Escherichia coli as an expressing system. The receptor belongs to the transferase category with E.C number 2.7.10.1. It has one chain with 337 amino acids [57].

3GOP. 3GOP is the crystal structure of the EGFR juxtamembrane and kinase domains. The receptor was isolated from *Homo sapiens* with *Spodoptera frugiperda* as an expressing system. The receptor belongs to the transferase category with E.C number 2.7.10.1. It has one chain with 361 amino acids [58].

4LQM. 4LQM is the crystal structure of EGFR L858R in complex with the ligand molecule N-[4-(3-Bromo-phenylamino)-quinazolin-6-yl]-acrylamide.The receptor was isolated from *Homo sapiens* with *Spodoptera frugiperda* as an expressing system. The receptor belongs to the transferase category with E.C number 2.7.10.1. It has one chain with 331 amino acids [59].

4R3R. 4R3R is the crystal structure of EGFR in complex with Mig6. The receptor was isolated from *Homo sapiens* with *Spodoptera frugiperda* as an expressing system. The receptor belongs to the transferase category with E.C number 2.7.10.1. It has one chain with 323 amino acids [60].

4ZJV. 4ZJV is the crystal structure of the EGFR kinase domain in a complex with the peptide-linking protein. The receptor was isolated from *Homo sapiens* with *Spodoptera frugiperda* and *Escherichia coli* as expression systems. The receptor belongs to the transferase category with E.C number 2.7.10.1.

5XWD. 5XWD is the crystal structure of the complex of 059-152-Fv fragment and EGFR-ECD complexed with 2-acetamido-2-deoxy-β-D-glucopyranose. The receptor was isolated from *Homo sapiens* with *Homo sapiens* as an expressing system. The receptor belongs to the signalling protein category with E.C number 2.7.10.1. It has one chain with 651 amino acids.

Tyrosine Kinase: 3CS9 (Receptor PDB id) was Selected

3CS9. 3CS9 is a human tyrosine (ABL) kinase co-crystallized with nilotinib. The receptor was isolated from *Homo sapiens* with *Spodoptera frugiperda* as an expressing system. The receptor belongs to the transferase category with E.C number 2.7.10.2. It has four chains with 277 amino acids on each chain.

Mitogen-activated Protein kinase-1: 3EQG and 4LMN (Receptor PDB id) were Selected

3EQG. 3EQG is the crystal structure of human MEK1 in a ternary complexed with N-{[(2R)-2,3- dihydroxy-propyl]oxy}-3,4-difluoro-2-[(2-fluoro-4-iodophenyl)amino] benzamide. The receptor was isolated from *Homo sapiens* with *Escherichia coli* as an expressing system. The receptor belongs to the transferase category with E.C number 2.7.12.2. It has one chain with 360 amino acids.

4LMN. 4LMN is a crystal Structure of MEK1 kinase receptor complexed with [3,4-bis(fluoranyl)-2-[(2-fluoranyl-4-iodanyl-phenyl)amino]phenyl]-[3-oxidanyl-3-[(2S)-piperidin-2-yl]azetidin-1-yl]methanone. The receptor was isolated from *Homo sapiens* with *Escherichia coli* as an expressing system. The receptor belongs to the transferase category with E.C number 2.7.12.2. It has one chain with 341 amino acids.

Estrogen Receptor Alpha: 3ERT (Receptor PDB id) was Selected

3ERT. 3ERT is a human estrogen receptor alpha complexed with 4-hydroxy tamoxifen. The receptor was isolated from *Homo sapiens* with *Escherichia coli* as an expressing system. The receptor belongs to the nuclear receptor category. It has one chain with 261 amino acids.

Cyclic Adenosine Monophosphate Dependent Kinase: 3OVV (Receptor PDB id) was Selected

3OVV. 3OVV is a human cyclic adenosine monophosphate-dependent protein kinase enzyme complexed with N'-[(1E)-(4-hydroxyphenyl) methylidene]-2-(3-methoxyphenyl) acetohydrazide inhibitor. The receptor was isolated from *Homo sapiens* with *Escherichia coli* as an expressing system. The receptor belongs to the transferase category with E.C number 2.7.11.11. It has one chain with 351 amino acids [61].

Peptidylprolyl Isomerase: 4DRH (Receptor PDB id) was Selected

4DRH. 4DRH is the crystallized structure of the peptidylprolyl isomerase domain of FKBP51, Rapamycin, and the FRB fragment of the mammalian target of rapamycin at low pH. The receptor was isolated from *Homo sapiens* with *Escherichia coli* BL21 as an expressing system. The receptor belongs to the isomerase/transferase category with E.C number 5.2.1.8. It has four chains with 144 amino acids (A and D chains) and 98 amino acids (B and E chains) [62].

Progesterone Receptor: 4OAR (Receptor PDB id) was Selected

4OAR. 4OAR is a progesterone receptor bound with [(8S,11R,13S,14S,17R)-17-acetyl-11-[4-(dimethylamino) phenyl]-13-methyl-3-oxo-1,2,6,7,8,11,12,14,15,16-deca-hydrocyclopenta[a]-phenanthren-17-yl] acetate as ligand molecule. The receptor was isolated from *Homo sapiens* with *Escherichia coli* BL21 as an expressing system. The receptor belongs to the transcription/peptide category. It has one chain with 258 amino acids [63].

Forkhead M1 DNA: 3G73 (Receptor PDB id) was Selected

3G73. 3G73 is the crystal structure of forkhead box protein M1 DNA binding protein. The receptor was isolated from *Homo sapiens* with *Escherichia coli* as an expressing system. The receptor belongs to the transcription DNA category. It has two chains with 142 amino acids on each chain [64].

Caspase Enzyme: 1QTN and 2XYP (Receptor PDB id) were Selected

1QTN. 1QTN is a crystal structure of caspase-8 complexed with tetrapeptide inhibitor. The receptor was isolated from *Homo sapiens* with *Escherichia coli* as an expressing system. The receptor belongs to the hydrolase category with E.C number 3.4.22. It has one chain with 164 amino acids.

2XYP. 2XYP is a crystal structure of caspase-3 complexed with phenylmethyl-N-[(2S)-4-chloro-3-oxo-1-phenyl-butan-2-yl] carbamate as an inhibitor. The receptor was isolated from *Homo sapiens* with *Escherichia coli* as an expressing system. The receptor belongs to the hydrolase category with E.C number 3.4.22.56. It has one chain with 146 amino acids [65].

Human Epidermal Growth fFactor 2: 3PP0 (Receptor PDB id) was Selected

3PP0. 3PP0 is a crystal structure of the Human HER2 kinase domain with 2-{2-[4-({5-chloro-6-

[3-(trifluoromethyl) phenoxy] pyridin-3-yl}amino)-5H-pyrrolo[3,2-d]pyrimidin-5 yl] ethoxy} ethanol inhibitor. The receptor was isolated from *Homo sapiens* with *Escherichia coli* as an expressing system. The receptor belongs to the transferase category with E.C number 2.7.10.1. It has one chain with 146 amino acids.

Cyclin-dependent Kinase 2/cyclin A: 4FX3 (Receptor PDB id) was Selected

4FX3. 4FX3 is a crystal Structure of the cyclin-dependent kinase 2/cyclin A complex with oxindole inhibitor (3Z)-2-oxo-3-[2-(4-sulfamoylphenyl)hydrazinylidene]-2,3-dihydro-1H-indole-5-carboxylic acid. The receptor was isolated from *Homo sapiens* with *Spodoptera frugiperda* as an expressing system. The receptor belongs to the transferase category with E.C number 2.7.11.22. It has four chains with 298 amino acids (A and C chains) and 258 amino acids (B and D chains).

Hepatitis C Virus Polymerase: 3HVO (Receptor PDB id) was Selected

3HVO. 3HVO is the structure of the genotype 2B hepatitis C virus polymerase complexed with 2-(3-bromophenyl)-6-[(2-hydroxyethyl)amino]-1H-benzo[de] isoquinoline-1,3(2*H*)-dione. The receptor was isolated from the *Hepatitis C virus isolate HC-J8* with *Escherichia coli* as an expressing system. The receptor belongs to the transferase category with E.C number 2.7.7.48. It has two chains with 563 amino acids on each chain.

Vascular Endothelial Growth Factor Receptors: 4AG8 and 2OH4 (Receptor PDB id) were Selected

4AG8. 4AG8 is a crystal structure of the VEGFR2 kinase domain in complex with axitinib. The receptor was isolated from *Homo sapiens* with *Spodoptera frugiperda* as an expressing system. The receptor belongs to the transferase category with E.C number 2.7.10.1. It has one chain with 316 amino acids.

2OH4. 2OH4 is the crystal structure of VEGFR2 with a benzimidazole-urea inhibitor (methyl (5-{4-[({[2-fluoro-5-(trifluoromethyl)phenyl]amino}carbonyl)amino]phenoxy}-1H-benzimidazol-2-yl)-carbamate). The receptor was isolated from *Homo sapiens* with *Escherichia coli* as an expressing system. The receptor belongs to the transferase category with E.C number 2.7.10.1. It has one chain with 316 amino acids [48].

Ligand Preparation

The structure of geniposidicacid was developed using Avogadro software. The molecule was optimized using MMFF94 and steepest descent methods. Then all the three-dimensional coordinates were added to the structure using Open Babel software. The total energy of the ligand was minimized using a swiss pdb viewer with the 20 steepest decent processes. Then all the polar hydrogens and gasteiger charges were added to the ligand molecule using AUTODOCK Vina and saved in PDB format.

Software Used in Molecular Docking Studies

In this manuscript, different software such as AUTODOCK VINA, Drug Discovery Studio 3.5 client, open Babel GUI, and Pymol were used [66].

Molecular Docking Parameters of Geniposidic Acid Interacted with Different Oncogenic Targets

All the water molecules and co-crystallized ligands were eliminated before performing a docking study. All the grid parameters were put in Table S1. The grid space of all the receptors was size_x = 24, size_y = 24, size_z = 24, and exhaustiveness = 8. All the receptors were energy minimized using swiss pdb viewer with 20 steepest decent.

Molecular Dynamics Simulation of Protein-ligand Complex

Molecular dynamic simulation data helped to understand the structural atomic level dynamics of the ligand molecules upon interaction with the receptors. In this study, the GROMACS 20.1 software package running on the LINUX UBUNTU platform was used to study the thermodynamic characteristics of the ligand-receptor complex. Separate the ligand molecule from the protein-ligand complex before beginning the simulation study, and then prepare GROMCAS-compatible gro files with the CHARMM 36 force field. Then TIP3P water molecules, solvent molecules, sodium, and chloride ions were added to the processed files. Then the processed files were energy minimized using the steepest descent algorithm process with 500,000 iterative steps with variable time factors (ps). The energy minimization process was processed in two distinct steps. In

the initial step, the number of particles, volume, and temperature (NVFT) remained constant, followed by choosing the number of particles, pressure, and temperature factors as constant. In this study, pressure (1 ATM) and temperature (298 °K) were used. After performing the simulation study, root mean square deviation (RMSD), root mean square fluctuation (RMSF), radius of gyration (R_g), solvent accessible surface area (SASA), Lennard-Jones short range and coulombic short range energy potentials were calculated. In the determination of the RMSD value, only movable heavy atoms were taken to identify the best pose. The lower bound and upper bound RMSD values were used to calculate the total molecule simulation. RMSD and RMSF calculations were performed by using the backbone of protein and Cα of protein, respectively. Whereas the structural integrity of the ligand-protein complex was determined by the radius of gyration, SASA represented the topological surface area of the receptor molecule exposed to the solvent molecule during the simulation process. The Lennard-Jones short-range and coulombic short-range energy potential calculations were performed to calculate the nonbonded energy.

Density Functional Theory Calculation of Geniposidic Acid

The density functional theory calculation of geniposidic acid was performed at the Becke-Lee-Parr hybrid exchange-correlation three-parameter functional (B3LYP) level with the standard 6-311G+(d,p) basis set. The complete geometry optimization and vibrational frequencies were calculated at the B3LYP/6-311G+(d,p) level on the basis of the optimized structure. Vibration analysis showed that the optimized structure was in accordance with the minimum points on the potential energy surface [67]. All the convergent precisions were the system default values, and all calculations reported in this work were carried out using the Avogadro-ORCA software combination. A HOMO-LUMO image of geniposidic acid was presented using IBOView software.

Profiling of Geniposidic Acid Using OSIRIS-MOLINSPIRATION

In-silico prediction of cLogP, solubility, molecular weight, topological polar surface area, drug-likeness, drug score, mutagenic risk, tumorigenic risk, irritant risk, and reproduction risk of geniposidic acid were assessed by OSIRIS software, and in-silico bioactivity of geniposidic acid was predicted by MOLINSPIRATION software [68].

RESULTS

Molecular Docking of Geniposidic Acid with Different Oncogenic Targets

Epidermal growth factor receptor tyrosine kinase. Geniposidic acid was docked with nine epidermal growth factor receptor tyrosine kinase receptors (PDB id: 1M17, 2J6M, 3QWQ, 4HJO, 3GOP, 4LQM, 4R3R, 4ZJV, and 5XWD). The ligand showed well docked against all the receptors with a good docking score. The binding energies of the molecule against 1M17, 2J6M, 3QWQ, 4HJO, 3GOP, 4LQM, 4R3R, 4ZJV and 5XWD were (-) 7.1 kcal mol^{-1}, (-) 8.0 kcal mol^{-1}, (-) 6.1 kcal mol^{-1}, (-) 9.0 kcal mol^{-1}, (-) 6.2 kcal mol^{-1}, (-) 8.2 kcal mol^{-1}, (-) 6.3 kcal mol^{-1}, (-) 7.5 kcal mol^{-1} and (-) 5.9 kcal $mol^{-1}$with LYS 721 2.0 Å, ASP 813 2.8 Å, ARG 817 2.8 Å by hydrogen bonding; MET 793 2.4 Å, ASP 855 2.0 Å by hydrogen bonding; ASN 389 2.4 Å, GLU 388 2.5 Å by hydrogen bonding and PRO 365 2.5 Å by pi-pi interactions; LYS 721 1.5 Å by hydrogen bonding and VAL 702, ALA 719, LEU 820 by pi-pi interactions; ASP 813 2.8 Å, ARG 817 2.1 Å, THR 766 2.7 Å by hydrogen bonding and ALA 719 by pi-pi interactions; LYS 745 2.0 Å, GLN 791 2.0 Å, MET 793 1.9 Å by hydrogen bonding and VAL 726, ALA 743 by pi-pi interactions; LYS 745 1.9 Å, and ASP 837 2.1 Å by hydrogen bonding; ASP 837 1.9 Å, CYS 390 2.7 Å by hydrogen bonding and PHE 723, PHE 856, ARG 841 by pi-pi interactions and ARG 285 2.5 Å, ASN 274 2.7 Å, VAL 6 2.1 Å, LYS 4 2.0 Å, MET 30 2.2 Å by hydrogen bonding; respectively (Fig. 2).

Tyrosine Kinase

Geniposidic acid was docked with the tyrosine kinase receptor (PDB id: 3CS9). The ligand molecule was well-docked against all the receptors with a good docking score. The binding energy of the molecule against 3CS9 was (-) 7.1 kcal mol^{-1} with ASP 381 2.2 Å, ARG 362 2.5 Å, HIS 361 2.6 Å by hydrogen bonding, and PHE 359 by pi-pi interaction (Fig. 3).

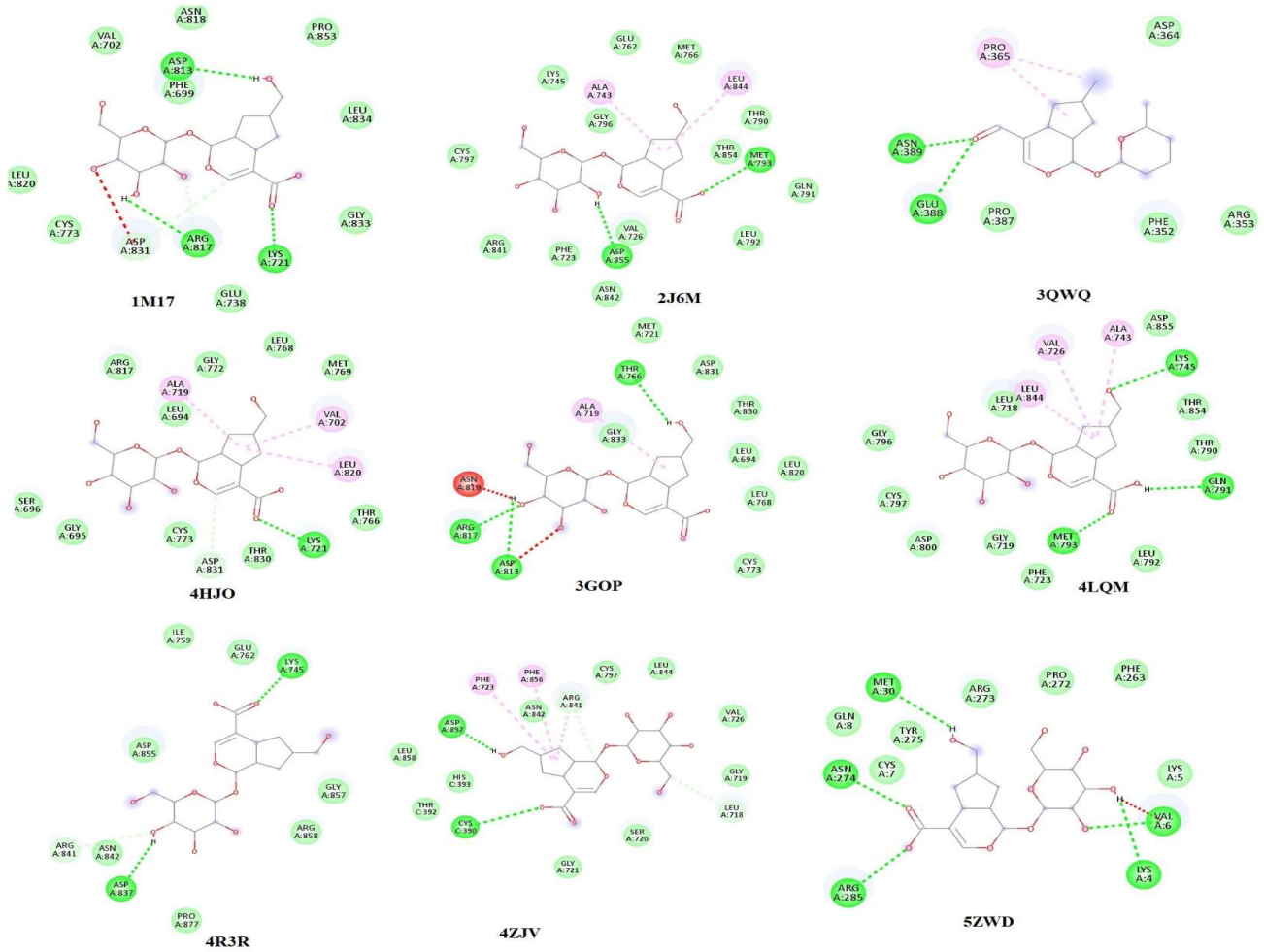

Fig. 2. Molecular docking interaction between geniposidic acid and receptors related to epidermal growth factor receptor tyrosine kinase.

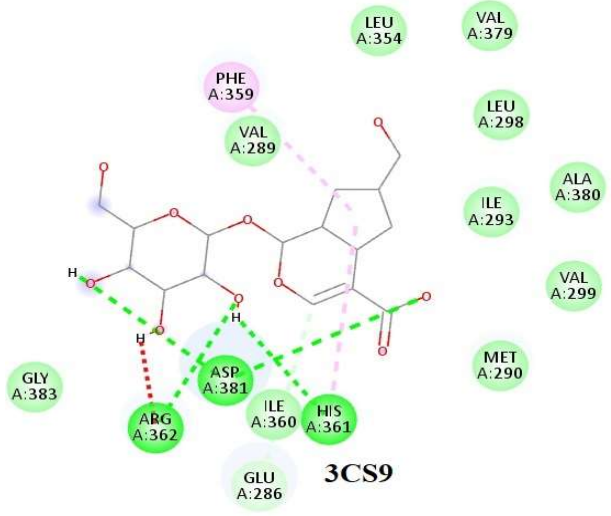

Fig. 3. Molecular docking interaction between geniposidic acid and receptors related to tyrosine kinase.

Mitogen-Activated Protein Kinase-1

Here, geniposidic acid was docked with two mitogen-activated protein kinase-1 receptors (PDB id: 3EQG and 4LMN). The ligand molecule was well-docked against all the receptors with a good docking score. The binding energies of the molecule against 3EQG and 4LMN were (-) 8.3 kcal mol^{-1} and (-) 8.2 kcal mol^{-1} with ASP 208 2.4 Å by hydrogen bonding and GLN 153 2.6 Å, SER 194 2.1 Å, MET 143 2.1 Å, and LYS 97 2.6 Å by hydrogen bonding; respectively Fig. 4).

Estrogen Receptor Alpha

Here, geniposidic acid was docked with estrogen receptor alpha receptor (PDB id: 3ERT). The ligand molecule was well-docked against all the receptors with a good docking score. The binding energy of the molecule against 3ERT was

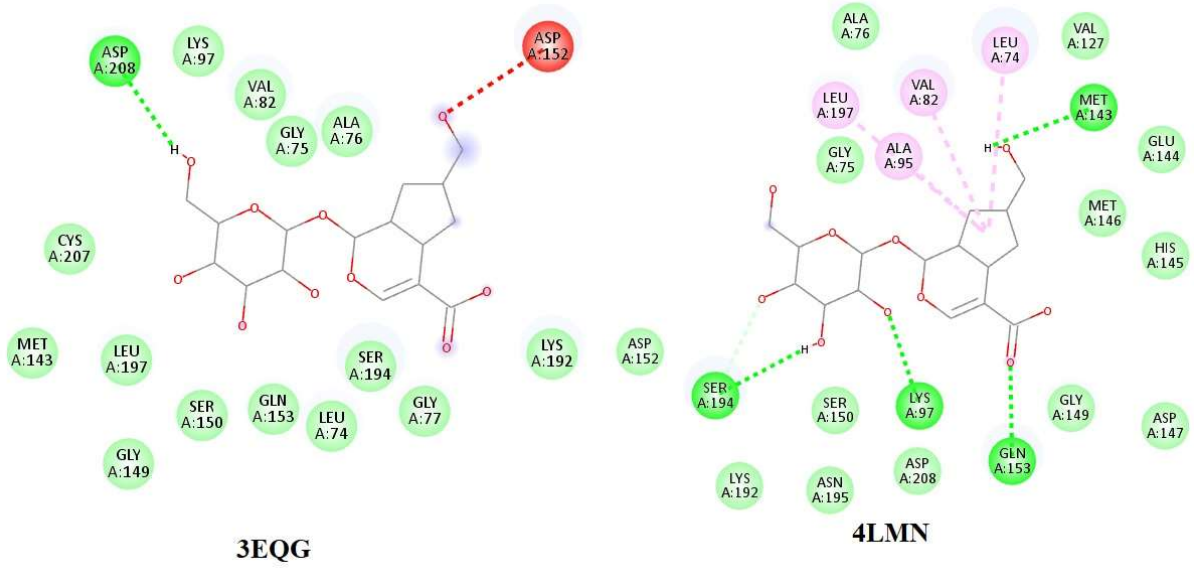

Fig. 4. Molecular docking interaction between geniposidic acid and receptors related to mitogen activated protein kinase-1.

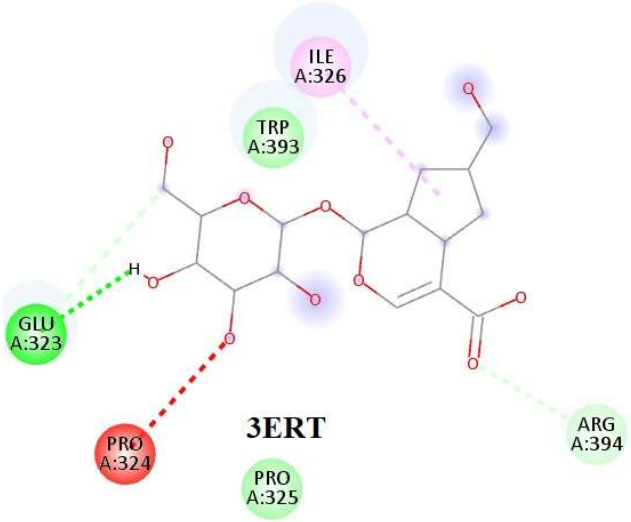

Fig. 5. Molecular docking interaction between geniposidic acid and receptors related to estrogen receptor alpha.

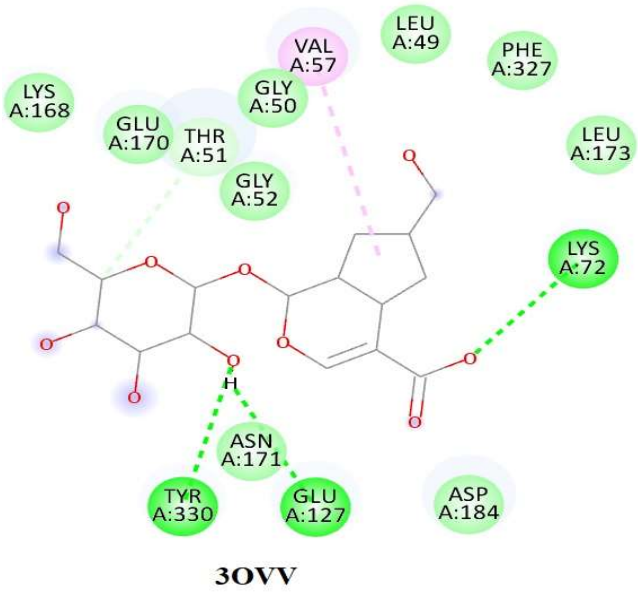

Fig. 6. Molecular docking interaction between geniposidic acid and receptors related to cyclic adenosine monophosphate dependent kinase.

(-) 5.1 kcal mol^{-1} with GLU 323 2.3 Å by hydrogen bonding and ARG 394 2.0 Å by van der Waal interaction (Fig. 5).

Cyclic Adenosine Monophosphate-dependent Kinase

Geniposidic acid was docked with the cyclic adenosine monophosphate-dependent kinase receptor (PDB id: 3OVV). The ligand molecule was well-docked against all the receptors with a good docking score. The binding energy of the molecule against 3OVV was (-) 7.8 kcal mol^{-1} with LYS 72 2.5 Å, GLU 127 2.5 Å, TYR 330 2.5 Å by hydrogen bonding, THR 51 by van der Waal, and VAL 57 by pi-pi interactions (Fig. 6).

Peptidylprolyl Isomerase

Geniposidic acid was docked with the peptidylprolyl isomerase receptor (PDB id: 4DRH). The ligand molecule was well-docked against all the receptors with a good docking score. The binding energy of the molecule against 4DRH was (-) 9.4 kcal mol^{-1} with THR 2098 2.4 Å, ASP 2102 2.1 Å, SER 2035 2.5 Å by hydrogen bonding, and TRP 2101, TYR 2105 by pi-pi interactions (Fig. 7).

Progesterone Receptor

Geniposidic acid was docked with the progesterone receptor (PDB id: 4OAR). The ligand molecule was well-docked against all the receptors with a good docking score. The binding energy of the molecule against 4OAR was (-) 8.5 kcal mol^{-1} with GLN 725 2.2 Å, GLU 695 2.6 Å by hydrogen bonding, and ILE 699 by pi-pi interactions (Fig. 8).

Forkhead M1 DNA

Geniposidic acid was docked with the forkhead M1 DNA receptor (PDB id: 3G73). The ligand molecule was well-docked against all the receptors with a good docking score. The binding energy of the molecule against 3G73 was (-) 6.1 kcal mol^{-1} with ASP 261 2.3 Å by hydrogen bonding and TRP 265 by pi-pi interactions (Fig. 9).

Caspase Enzyme

Geniposidic acid was docked with two caspase enzyme receptors (PDB id: 1QTN and 2XYP). The ligand molecule was well-docked against all the receptors with a good docking score. The binding energies of the molecule against 1QTN and 2XYP were (-) 5.6 kcal mol^{-1} and (-) 5.7 kcal mol^{-1} with GLU 290 2.6 Å by hydrogen bonding and TYR 293 by pi-pi interaction and ILE 160 2.4 Å by pi-pi interaction and GLY 125 2.4 Å by van der Waal interaction; respectively (Fig. 10).

Human Epidermal Growth Factor-2

Geniposidic acid was docked with the human epidermal growth factor-2 receptor (PDB id: 3PP0). The ligand molecule was well-docked against all the receptors with a good docking score. The binding energy of the molecule against 3PP0 was (-) 5.7 kcal mol^{-1} with SER 728 2.0 Å, ARG 849 2.8 Å, GLY 729 2.4 Å, ASP 845 2.8 Å by hydrogen bonding (Fig. 11).

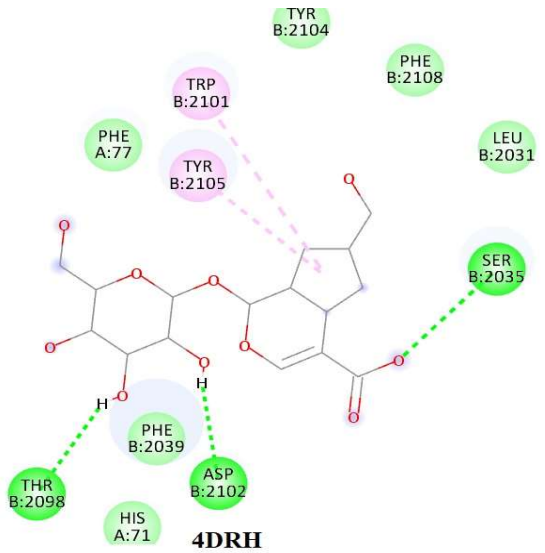

Fig. 7. Molecular docking interaction between geniposidic acid and receptors related to peptidylprolyl isomerase.

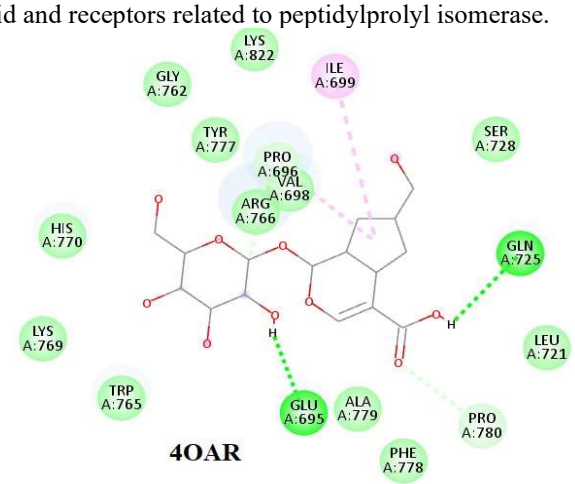

Fig. 8. Molecular docking interaction between geniposidic acid and receptors related to progesterone receptor.

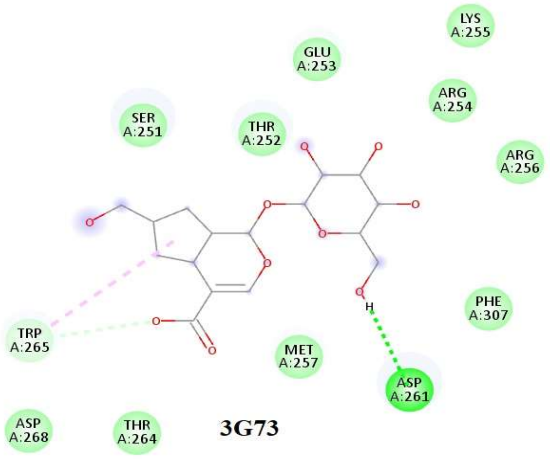

Fig. 9. Molecular docking interaction between geniposidic acid and receptors related to forkhead M1 DNA.

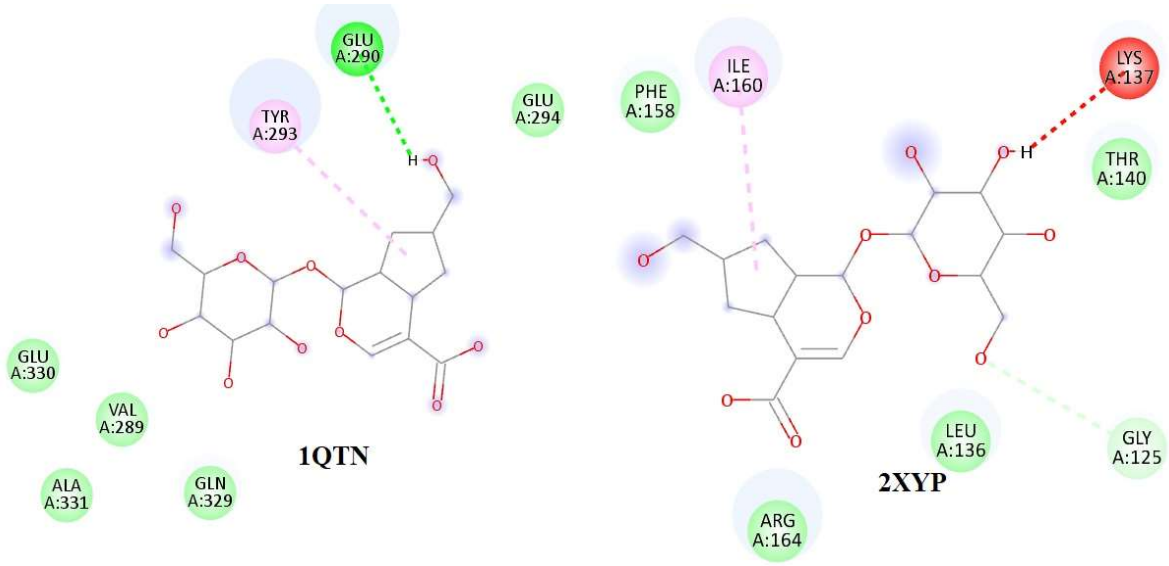

Fig. 10. Molecular docking interaction between geniposidic acid and receptors related to caspase enzyme.

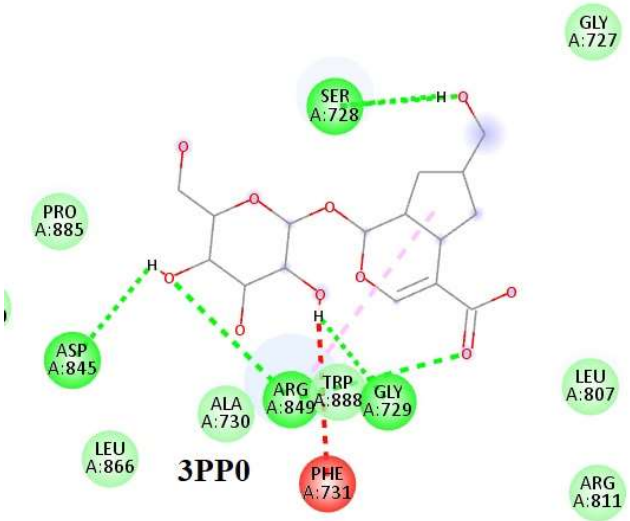

Fig. 11. Molecular docking interaction between geniposidic acid and receptors related to human epidermal growth factor 2.

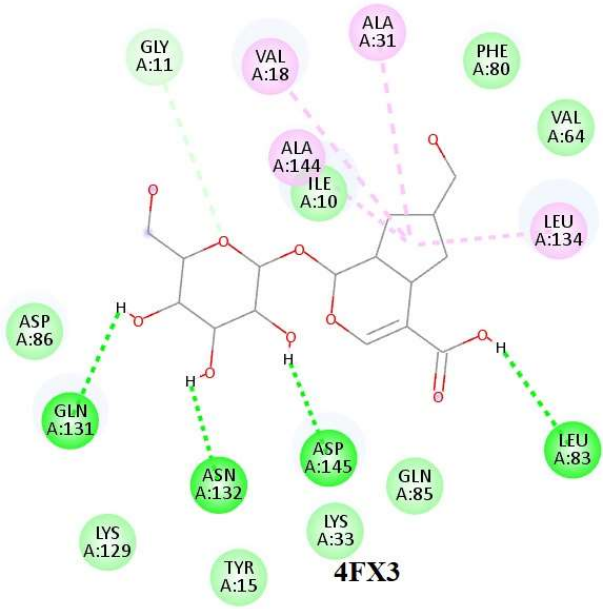

Fig. 12. Molecular docking interaction between geniposidic acid and receptors related to cyclin-dependent kinase 2/cyclin A.

Cyclin-Dependent Kinase 2/Cyclin A

Geniposidic acid was docked with cyclin-dependent kinase 2/cyclin A receptor (PDB id: 4FX3). The ligand molecule was well-docked against all the receptors with a good docking score. The binding energy of the molecule against 4FX3 was (-) 7.5 kcal mol^{-1} ASP 145 2.1 Å, GLN 131 2.8 Å, ASN 132 2.4 Å, LEU 83 2.8 Å by hydrogen bonding (Fig. 12).

Hepatitis C Virus Polymerase

Geniposidic acid was docked with the hepatitis C virus

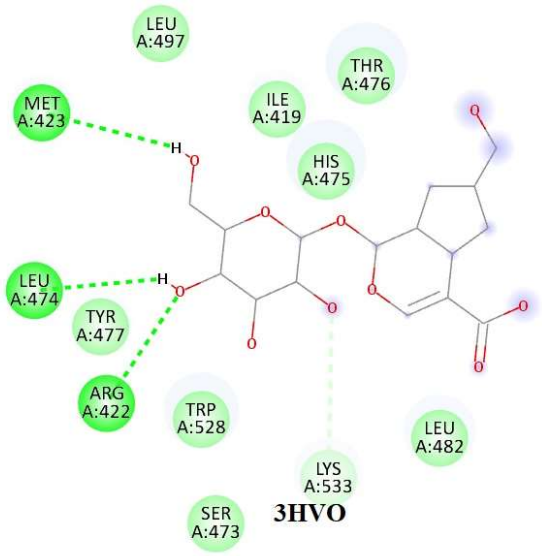

Fig. 13. Molecular docking interaction between geniposidic acid and receptors related to hepatitis c virus polymerase.

polymerase receptor (PDB id: 3HVO). The ligand molecule was well-docked against all the receptors with a good docking score. The binding energy of the molecule against 3HVO was (-) 5.9 kcal mol^{-1} with ARG 422 2.6 Å, MET 423 2.5 Å, LEU 474 2.7 Å by hydrogen bonding (Fig. 13).

Vascular Endothelial Growth Factor Receptor

Geniposidic acid was docked with two vascular endothelial growth factor receptors (PDB id: 4AG8 and 2OH4) related to VEGFR. The ligand molecule was well-docked against all the receptors with a good docking score. The binding energies of the molecule against 4AG8 and 2OH4 were (-) 9.2 kcal mol^{-1} and (-) 8.0 kcal mol^{-1} with ASP 1046 2.3 Å by hydrogen bonding and VAL 899, CYS 1045 by pi-pi interactions, and GLU 883 2.7 Å, ASP 1044 2.3 Å by hydrogen bond and ILE 886 by pi-pi interaction, respectively (Fig. 14).

All the molecular docking interactive binding energy and surrounding residues of geniposidic acid with different cancer-related receptors were tabulated in Table 1.

Molecular Dynamic Simulations of Geniposidic Acid Interacted with Oncogenic Targets

After performing molecular dynamic simulations of the docked conformers: root mean square deviation (RMSD), root mean square fluctuation (RMSF), the radius of gyration (Rg), solvent accessible surface area (SASA), Lennard-Jones short range (kJ mol^{-1}) and coulombic-short range (kJ mol^{-1}) interaction energies were determined (Table 2).

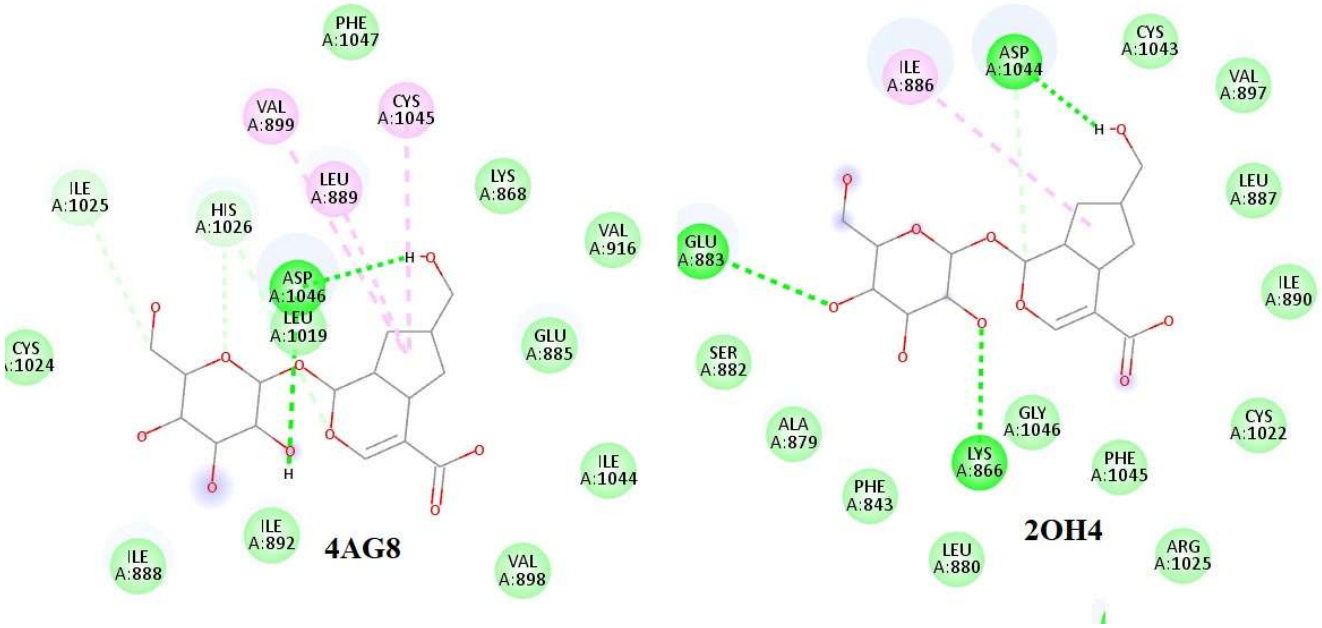

Fig. 14. Molecular docking interaction between geniposidic acid and receptors related to vascular endothelial growth factor receptor.

Table 1. Molecular Docking Gtudies Data on the Interaction between Geniposidic Acid and Different Oncogenic Targets

SN	Receptors PDB id.	Binding energy (Kcal mol^{-1})	Interactive residues with 4.0 Å
Receptors related to Epidermal Growth Factor Receptor Tyrosine Kinase			
1	1M17	(-) 7.1	LYS 721 2.0 Å, ASP 813 2.8 Å, ARG 817 2.8 Å by hydrogen bonding
2	2J6M	(-) 8.0	MET 793 2.4 Å, ASP 855 2.0 Å by hydrogen bonding
3	3QWQ	(-) 6.1	ASN 389 2.4 Å, GLU 388 2.5 Å by hydrogen bonding and PRO 365 2.5 Å by pi-pi interaction
4	4HJO	(-) 9.0	LYS 721 1.5 Å by hydrogen bonding and VAL 702, ALA 719, LEU 820 by pi-pi interactions
5	3GOP	(-) 6.2	ASP 813 2.8 Å, ARG 817 2.1 Å, THR 766 2.7 Å by hydrogen bonding and ALA 719 by pi-pi interactions
6	4LQM	(-) 8.2	LYS 745 2.0 Å, GLN 791 2.0 Å, MET 793 1.9 Å by hydrogen bonding and VAL 726, ALA 743 by pi-pi interactions
7	4R3R	(-) 6.3	LYS 745 1.9 Å, and ASP 837 2.1 Å by hydrogen bonding
8	4ZJV	(-) 7.5	ASP 837 1.9 Å, CYS 390 2.7 Å by hydrogen bonding and PHE 723, PHE 856, ARG 841 by pi-pi interactions
9	5XWD	(-) 5.9	ARG 285 2.5 Å, ASN 274 2.7 Å, VAL 6 2.1 Å, LYS 4 2.0 Å, MET 30 2.2 Å by hydrogen bonding
Receptor related to Tyrosine Kinase			
1	3CS9	(-) 7.1	ASP 381 2.2 Å, ARG 362 2.5 Å, HIS 361 2.6 Å by hydrogen bonding and PHE 359 by pi-pi interaction
Receptors related to Mitogen Activated Protein Kinase-1			
1	3EQG	(-) 8.3	ASP 208 2.4 Å by hydrogen bonding
2	4LMN	(-) 8.2	GLN 153 2.6 Å, SER 194 2.1 Å, MET 143 2.1 Å, and LYS 97 2.6 Å by hydrogen bonding
Receptor related to Estrogen Receptor Alpha			
1	3ERT	(-) 5.1	GLU 323 2.3 Å by hydrogen bonding and ARG 394 2.0 Å by van der Waal interaction
Receptor related to Cyclic Adenosine Monophosphate dependent kinase			
1	3OVV	(-) 7.8	LYS 72 2.5 Å, GLU 127 2.5 Å, TYR 330 2.5 Å by hydrogen bonding, THR 51 by van der Waal interaction and VAL 57 by pi-pi interaction
Receptor related to Peptidylprolyl Isomerase			
1	4DRH	(-) 9.4	THR 2098 2.4 Å, ASP 2102 2.1 Å, SER 2035 2.5 Å by hydrogen bonding and TRP 2101, TYR 2105 by pi-pi interactions
Receptor related to Progesterone Receptor			
1	4OAR	(-) 8.5	GLN 725 2.2 Å, GLU 695 2.6 Å by hydrogen bonding and ILE 699 by pi-pi interaction
Receptor related to Forkhead M1 DNA			
1	3G73	(-) 6.1	ASP 261 2.3 Å by hydrogen bonding and TRP 265 by pi-pi interaction
Receptors related to Caspase Enzyme			
1	1QTN	(-) 5.6	GLU 290 2.6 Å by hydrogen bonding and TYR 293 by pi-pi interaction
2	2XYP	(-) 5.7	ILE 160 2.4 Å by pi-pi interaction and GLY 125 2.4 Å by van der Waal interaction
Receptor related to Human Epidermal Growth Factor 2			
1	3PP0	(-) 5.7	SER 728 2.0 Å, ARG 849 2.8 Å, GLY 729 2.4 Å, ASP 845 2.8 Å by hydrogen bonding
Receptor related to Cyclin-Dependent Kinase 2/Cyclin A			
1	4FX3	(-) 7.5	ASP 145 2.1 Å, GLN 131 2.8 Å, ASN 132 2.4 Å, LEU 83 2.8 Å by hydrogen bonding
Receptor related to Hepatitis C Virus Polymerase			
1	3HVO	(-) 5.9	ARG 422 2.6 Å, MET 423 2.5 Å, LEU 474 2.7 Å by hydrogen bonding
Receptors related to Vascular Endothelial Growth Factor Receptor			
1	4AG8	(-) 9.2	ASP 1046 2.3Å by hydrogen bonding and VAL 899, CYS 1045 by pi-pi interactions
2	2OH4	(-) 8.0	GLU 883 2.7 Å, ASP 1044 2.3 Å by hydrogen bonding and ILE 886 by pi-pi interaction

Table 2. Molecular Dynamics Simulation Data between Geniposidic Acid Interacted with Different Oncogenic Targets

SN	Receptors PDB id.	RMSD	RMSF	Lennard-Jones-Short Range: Protein-Ligand (kJ mol^{-1})	Coulombic-Short Range: Protein-Ligand (kJ mol^{-1})	Radius of gyration	SASA (nm\S^2\N)
Receptors related to Epidermal Growth Factor Receptor Tyrosine Kinase							
1	1M17	0.2975	0.0576-0.5866	-79.4825	-101.503	2.21-2.41	452.8437
2	2J6M	0.3011	0.0417-0.4065	-0.000130	-0.000225	1.95-1.99	324.562
3	3QWQ	0.3063	0.0677-0.3852	-4.48317	-2.88441	3.34-3.56	127.6683
4	4HJO	0.1382	0.0315-0.3736	-4.45317	-2.74441	2.12-2.35	85.3868
5	3GOP	0.3016	0.0441-0.9107	-0.286121	-0.541156	2.27-2.42	331.61
6	4LQM	0.1724	0.033- 0.2337	-0.00010650	-0.00055047	1.96-2.00	165.6271
7	4R3R	0.2003	0.0325-0.5216	-2.53327	-0.945977	1.99-1.98	294.9133
8	4ZJV	0.1518	0.0347-0.223	-0.00510159	-0.012342	1.88-1.93	155.0219
9	5XWD	0.3673	0.0767-0.3812	-1.045159	-8.125642	3.47-3.52	320.5454
Receptor related to Tyrosine Kinase							
1	3CS9	0.1329	0.0306-00.266	-138.172	-91.3755	1.86-1.90	320.6263
Receptors related to Mitogen Activated Protein Kinase-1							
1	3EQG	0.2490	0.0345-0.3349	-0.000258	-0.000556	1.94-1.98	165.5521
2	4LMN	0.2257	0.0424-0.4518	0.00000650	0.00002047	1.91-1.94	89.9716
Receptor related to Estrogen Receptor Alpha							
1	3ERT	0.1546	0.0389-0.6151	-0.603027	-0.115528	1.86-1.88	140.4818
Receptor related to Cyclic Adenosine Monophosphate dependent kinase							
1	3OVV	0.1256	0.0337-0.2068	-17.3512	-22.8906	1.98-2.01	186.738
Receptor related to Peptidylprolyl Isomerase							
1	4DRH	0.08234	0.0322-0.1515	-1.05314	-0.891433	1.29-1.30	50.7433
Receptor related to Progesterone Receptor							
1	4OAR	0.1614	0.0329-0.3254	-13.2273	-1.83977	1.83-1.82	134.835
Receptor related to Forkhead M1 DNA							
1	3G73	0.1167	0.0376-0.2146	-0.33231	-0.322150	1.30-1.31	52.6484
Receptors related to Caspase Enzyme							
1	1QTN	0.3619	0.0457-0.4709	-0.00008	-0.000103	1.72-1.66	85.32026
2	2XYP	0.2642	0.046-0.6888	-50.2643	-45.3019	1.72-1.77	82.59736
Receptor related to Human Epidermal Growth Factor 2							
1	3PP0	0.1521	0.0326-0.5216	-2.78376	-2.31893	1.89-1.94	156.7536
Receptor related to Cyclin-Dependent Kinase 2/Cyclin A							
1	4FX3	0.1126	0.0318-0.3104	18.0202	-9.52566	1.97-2.00	165.5521
Receptor related to Hepatitis C Virus Polymerase							
1	3HVO	0.1193	0.0321-0.1740	-8.63665	-4.5638	2.38-2.41	294.9133
Receptors related to Vascular Endothelial Growth Factor Receptor							
1	4AG8	0.1193	0.0307-0.2378	-91.5383	-71.8753	1.93-1.96	163.0534
2	2OH4	0.1751	0.0338-0.3811	-9.76441	-1.40951	1.99-2.01	165.6271

Data from the Geniposidic Acid DFT Calculation

The difference between the highest occupied molecular orbital (HOMO) and the lowest unoccupied molecular orbital (LUMO) was used to study the transfer of electrons participating in interaction by using frontier molecular orbitals. Chemical reactivity parameters such as global hardness (η), electronegativity (χ), chemical potential (μ), global softness (S), and global electrophilicity index (ω) were calculated. EHOMO, ELUMO, ΔE gap, IE, A, η, ω, χ, μ, S, σ, ionization potential (vertical) in the gas phase, total thermal energy, total enthalpy, Gibbs free energy values of geniposidic acid were -6.555 (eV), -1.027 (eV), 5.528 (eV), 6.555, 1.027, 2.764, 2.599, 3.791, -3.791, 0.181, 0.362, +6.555, -1374.55053115 (Eh), -1374.54958694 (Eh) and -1374.62774971 (Eh) respectively (Table 3).

Geniposidic Acid Data Using OSIRIS-MOLINSPIRATION

The *in-silico* bioactivity data revealed the bioactivity scores of geniposidic acid for GPCR ligand, Ion channel modulator, kinase inhibitor, nuclear receptor ligand, protease inhibitor, and enzyme inhibitor were 0.34, 0.32, (-) 0.02, 0.22, 0.21 and 0.68, respectively (Table 4). cLogP, solubility, molecular weight, topological polar surface area, drug-likeness, and drug score of geniposidic acid were -2.5, -0.66, 374.0, 166.1, -2.8, 0.48, respectively, without any possible mutagenic, reproductive, or tumorigenic toxicity (Table 5).

DISCUSSION

Molecular docking study data of geniposidic acid was observed with good docking interaction with 4DRH (-9.4 kcal mol^{-1}) followed by 4AG8 (- 9.2 kcal mol^{-1}) and 4HJO (-9.0 kcal mol^{-1}) (Fig. 15). The 4DRH receptor, as previously stated, is a peptidyl-prolyl isomerase enzyme that is bound to its inhibitor rapamycin [69,70]. Rapamycin (Sirolimus) successfully inhibited tumour growth by inhibiting angiogenesis and significantly reducing VEGF formation *via* the mTOR pathway [71]. Pin1 (Peptidyl-prolyl cis-trans isomerase NIMA-interacting1), cyclophilin, and FK506 protein binding domain are all associated with the peptidylprolyl isomerase enzyme [72]. Overexpression of peptidylprolyl isomerase and associated factors directly correlate with the occurrence and progression of cancer [73].

Table 3. DFT Calculation of Geniposidic Acid

1	E_{HOMO} (eV)	-0.2409
2	E_{LUMO} (eV)	-0.0377
3	ΔE gap (eV)	0.2032
4	IE	0.2409
5	A	0.0377
6	η	0.1016
7	ω	0.09549
8.	χ	0.1393
9	μ	-0.1393
10	S	4.92125
11	σ	9.84251
12	Ionization potential (vertical) in gas phase	7.42234
13	Total thermal energy (Eh)	-1374.55053115
14	Total enthalpy (Eh)	-1374.54958694
15	Gibbs free energy (Eh)	-1374.62774971

Table 4. Bioactivity Score of Geniposidic Acid

SN	Activity type	Bioactivity score
1	GPCR ligand	0.34
2	Ion channel modulator	0.32
3	Kinase inhibitor	-0.02
4	Nuclear receptor ligand	0.22
5	Protease inhibitor	0.21
6	Enzyme inhibitor	0.68

Table 5. OSIRIS Calculation of Geniposidic Acid

SN	clogP	- 2.5	++
1	Solubility	-0.66	++
2	MW	374.0	++
3	TPSA	166.1	-
4	Drug likeness	-2.8	-
5	Drug score	0.48	+
5	Mutagenic risk	No	++
6	Tumorigenic risk	No	++
7	Irritant risk	No	++
8	Reproductive risk	No	++

++Poistive impact; +need modification; -negative impact.

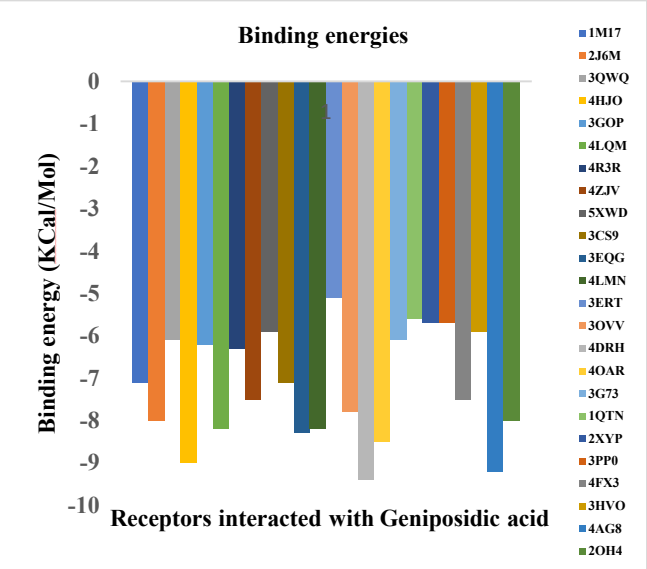

Fig. 15. Molecular docking binding energies interaction between geniposidic acid and different oncogenic targets.

Sulfopin, juglone, and aliporivir minimized the viability of ovarian, pancreatic, and liver cancer cells [74]. Among other interactive receptors, 4AG8 belongs to VEGFR2 with its inhibitor axitinib [75]. As we know, axitinib decreased the expression of interleukin-6, tumor necrosis factor-alpha, and interferon-gamma [76,77], which collectively suppressed the growth of skin cancer, lung cancer, and advanced staged kidney cancer, along with metastasizing renal carcinoma [78]. Among the top three interactive receptors, 4HJO was the last one associated with EGFR tyrosine kinase bound with its inhibitor, erlotinib. Erlotinib is mentioned in the treatment of non-small lung cancer and advanced pancreatic cancer [79]. Also, the interactive residues of geniposidic acid upon interaction with 4DRH, 4AG8, and 4HJO were like the surrounding residues of the complexed ligands (rapamycin, erlotinib, and axitinib). As geniposidic acid interacted with the receptor and docked in place of bound ligands, it was obvious that geniposidic acid would show its anticancer activity in the same manner as rapamycin, axitinib, and erlotinib [80]. The MD simulation data revealed that the RMSD values of the docked conformers were within (0.08234-0.3673, which confirmed that all the complexes were within the range of 2.0 Å. RMSF data showed some major fluctuations around 2000 and 3000 atoms, with a maximum value of 0.4 nm. Some big fluctuations were also observed around 2303, 2396, and 3986 atoms directly related to 1QTN, 2XYP, and 3ERT docked conformers. These fluctuations were observed due to the low number of amino acids present in the proteins (1QTN: 164 amino acids, 2XYP: 146 amino acids, and 3ERT: 261 amino acids). These RMSF data confirmed that all the ligand molecules interacted well with the receptor without disturbing the structural integrity (Fig. 16).

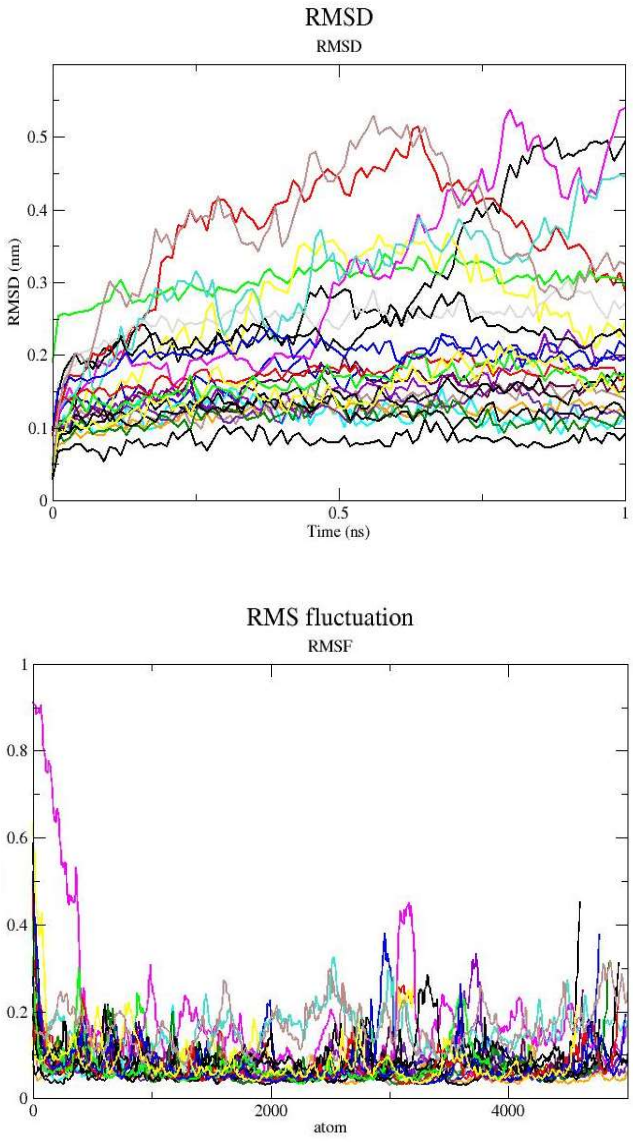

Fig. 16. MD simulation (RMSD and RMSF) data interaction between geniposidic acid and different oncogenic targets.

The radius of gyration data reflected the integrity of the protein-ligand complex. The gyration value maintained a steady flow for a stable structure and a fluctuation in an unfolded structure. A high gyration value reflected less stability, and a lower gyration value correlated with more stability of the protein structure. The Rg values of all the ligand-receptor complexes were within (0.0307-0.9927) nm. Gyration data confirmed the stability of the protein-ligand complex. The measurement of SASA values reflected the defined area of the target protein, which was a freely accessible area to the solvents during the simulation process. SASA values were found to be between (50.7433-452.8437) nm/S2/N. SASA data confirmed that ligand molecules did not have any negative effect on different foldings of the protein structure (Fig. 17).

As per both Lennard-Jones and short-range coulombic interaction energy data, all the protein-geniposidic complexes except the geniposidic acid-4LMN complex positively impacted on the ligand affinity towards the receptors [81].

The chemical reactivity of a molecule directly depends upon its orbital energy. Inside a molecule, an electron flows from an electron-rich HOMO to an electron-deficient LUMO. As per thermodynamics, negative values of HOMO (-0.2409 eV) and LUMO (-0.0377 eV), as well as a lower energy gap (ΔE) of 0.2032, stated the stable nature of geniposidic acid [82]. This low energy gap value makes the molecule soft, which confirms that the molecule easily donates an electron to an acceptor molecule. Also, geniposidic acid was observed to have a preferable ionisation value (I = 0.2409), ionization potential value (7.42234), chemical hardness value (η = 0.1016), and a global electrophilicity index (ω = 0.09549), which confirmed that geniposidic acid was stable and reactive [83]. Among other important parameters, the chemical potential (μ = -0.1393) value was also an important parameter to measure the stability of the compound. Frontier molecular orbital theory suggests that the biological activity of a molecule depends upon its HOMO and LUMO energy. As per the DFT calculation image, the HOMO orbital of geniposidic acid mainly delocalized on the total aglycone part, and in the case of the LUMO orbital image, the total electron cloud focused on the C-O-C=C-COOH group of the aglycone part (Fig. 18). These data confirmed that the aglycone part of geniposidic acid effectively participated in biological interactions. As we know, if the bioactivity score was more than 0.00, then the molecule became active; if the bioactivity score was between -0.50 to 0.00, then the molecule became moderately active, and finally, if the score was less than -0.50, then the molecule became inactive [84]. The outcomes revealed that geniposidic acid may show its activity prominently by inhibiting an enzyme followed by interacting with GPCR and

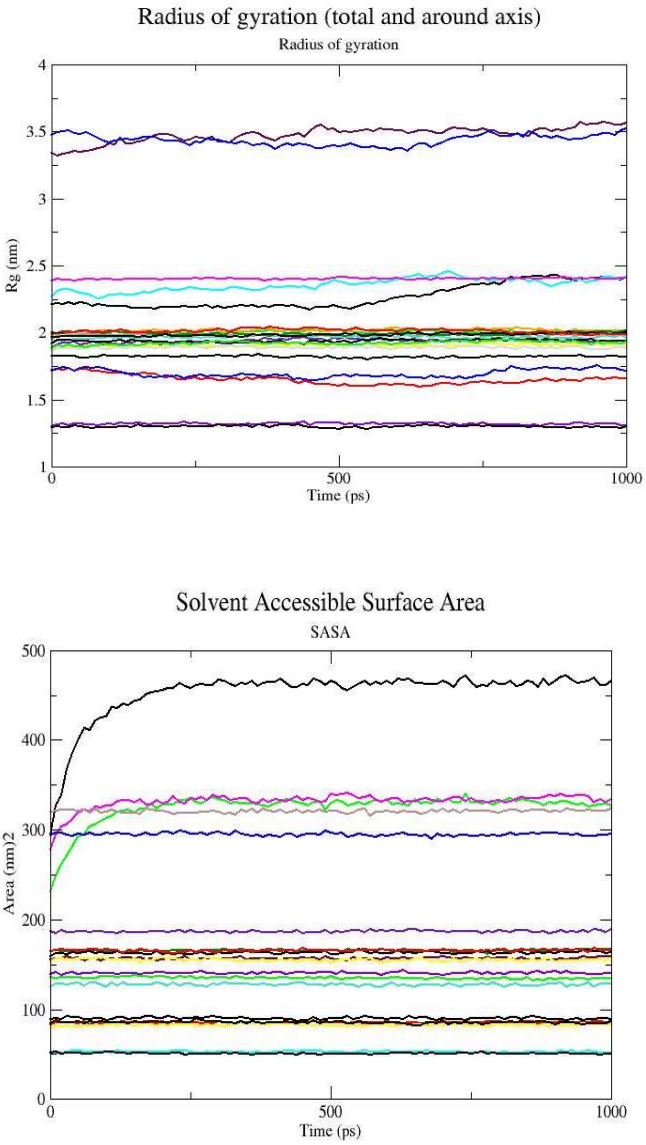

Fig. 17. MD simulation (Rg and SASA) data interaction between geniposidic acid and different oncogenic targets.

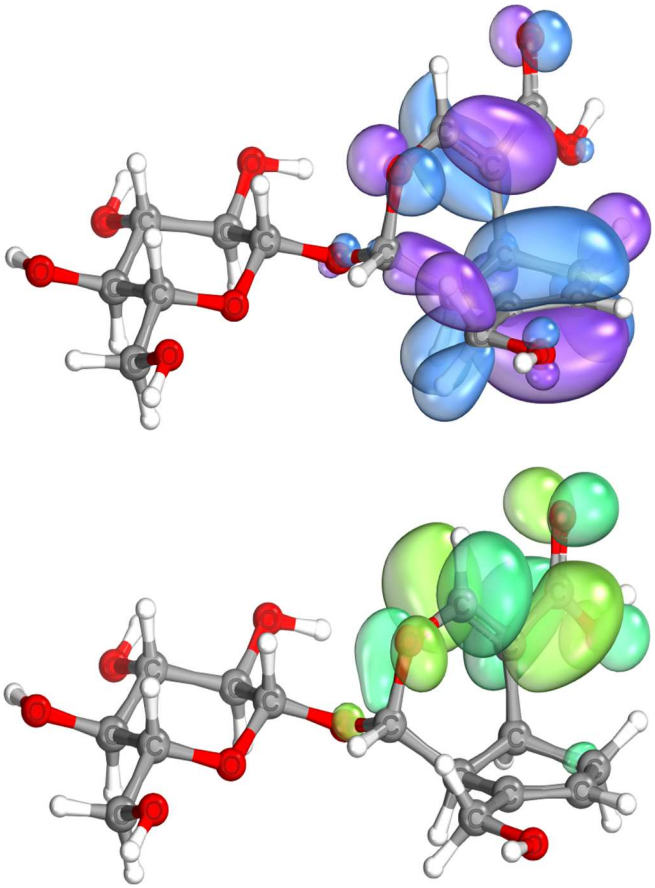

Fig. 18. HOMO and LUMO maps of geniposidic acid from DFT/B3LYP/6-311G+(d,p) calculation.

nuclear receptor ligands, modulating the ion channels [85]. Theoretical toxicity risk assessment of geniposidic acid revealed that the molecule did not show any toxicity and the drug score (0.48) confirmed that little modification in the structure produces a more effective molecule.

CONCLUSION

In molecular docking studies between geniposidic acid and various oncogenic targets, it was discovered that geniposidic acid docked well with 4DRH, 4AG8, and 4HJO. The interactive residues of geniposidic acid upon interaction with 4DRH, 4AG8, and 4HJO were like the surrounding residues of the complexed ligands (rapamycin, axitinib, and erlotinib). Molecular docking studies suggest that geniposidic acid shows anticancer activity by interacting with peptidylprolyl isomerase, VEGFR2, and EGFR tyrosine kinase. The MD simulation data suggested that all the docked complexes interacted well within the receptor active site without disturbing the structural integrity. The DFT calculation of geniposidic acid revealed that the aglycone part of the structure participated in the receptor interaction and other electronic parameters also supported the same. In the same way, OSIRIS-MOLINSPIRATION data showcased the positive factors of the molecule. This information collectively confirms that if we pharmacologically establish the molecule, then it will be a boon for mankind to treat cancer.

LIST OF ABBREVIATIONS

MAPK: Mitogen-Activated Protein Kinase; EGFR/HER: Human Epidermal Growth Factor Receptor; VEGFR: Vascular Endothelial Growth Factor Receptor; ErbB: Erythro Blastosis Oncogene B; TKIs: Tyrosine Kinase Inhibitors; EC: Enzyme Commission; MEK1: Mitogen-Activated protein Kinase1; ECD: Extra Cellular Domain; IGC_{50}: 50% Inhibition Growth Concentration; LC_{50}: Lethal Concentration 50%; LD_{50}: Lethal Dose 50%; RMSD: Relative Mean Standard Deviation; LYS: Lysine; VAL: Valine; GLU: Glutamic acid; PHE: Phenylalanine; CYS: Cysteine; ASP: Aspartic acid; MET: Methionine; LEU: Leucine; GLN: Glutamine; GLY: Glycine; ASN: Asparagine; SER: Serine; THR: Threonine; ARG: Arginine. PI3K/AKT: PhosphatidyInositol-3-Kinase/ Protein kinase B; cAMP: Cyclic Adenosine Mono Phosphate; ERK: Extracellular signal-regulated Kinase; JNK/p38MAPK: c-Jun N-terminal kinase/Mitogen-Activated Protein Kinase; CDK: Cyclin Dependent kinase; HCV: Hepatitis C Virus; HCC: Hepato Cellular Carcinoma; PDGF: Platelet-Derived Growth Factor.

REFERENCES

[1] Salehi, B.; Zucca, P.; Sharifi-Rad, M.; Pezzani, R.; Rajabi, S.; Setzer, W. N.; Varoni, E. M.; Iriti, M.; Kobarfard, F.; Sharifi-Rad, J., Phytotherapeutics in cancer invasion and metastasis. *Phytother. Res.*, **2018**, *32* (8), 1425-49. DOI: 10.1002/ptr.6087, PMID 29672977.

[2] Kaur, S.; Pandit, K.; Chandel, M.; Kaur, S.,

Antiproliferative and apoptogenic effects of Cassia fistula L. n-hexane fraction against human cervical cancer (HeLa) cells. *Environ. Sci. Pollut. Res. Int.,* **2020**, *27* (25), 32017-33. DOI: 10.1007/s11356-020-08916-9, PMID 32504442.

[3] Cancer statistics [cited Dec 15, 2020]. Available from: https://www.cancer.gov/aboutcancer/understanding/statistics.

[4] Shu, L.; Cheung, K. L.; Khor, T. O.; Chen, C.; Kong, A. N., Phytochemicals: cancer chemoprevention and suppression of tumor onset and metastasis. *Cancer. Metastasis. Rev.,* **2010**, *29* (3), 483-502. DOI: 10.1007/s10555-010-9239-y, PMID 20798979.

[5] Cainap, C.; Nagy, V.; Seicean, A.; Gherman, A.; Laszlo, I.; Lisencu, C.; Nadim, A. H.; Constantin, A. M.; Cainap, S., Results of third-generation epirubicin/cisplatin/xeloda adjuvant chemotherapy in patients with radically resected gastric cancer. *J. Buon.,* **2016**, *21* (2), 349-59. PMID 27273944.

[6] Irimie, A. I.; Braicu, C.; Cojocneanu-Petric, R.; Berindan-Neagoe, I.; Campian, R. S., Novel technologies for oral squamous carcinoma biomarkers in diagnostics and prognostics. *Acta. Odontol. Scand.,* **2015**, *73* (3), 161-8. DOI: 10.3109/00016357.2014.986754, PMID 25598447.

[7] Chiorean, R.; Braicu, C.; Berindan-Neagoe, I., Another review on triple negative breast cancer. Are we on the right way towards the exit from the labyrinth? *Breast.,* **2013**, *22* (6), 1026-33. DOI: 10.1016/j.breast.2013.08.007, PMID 24063766.

[8] Baell, J.; Walters, M. A., Chemistry: chemical con artists foil drug discovery. *Nature.,* **2014**, *513* (7519), 481-3. DOI: 10.1038/513481a, PMID 25254460.

[9] Baell, J. B.; Nissink, J. W. M., Seven yearitch: pan-assayinterferencecompounds (PAINS) in 2017-utility and limitations. *ACS. Chem. Biol*., **2018**, *13* (1), 36-44. DOI: 10.1021/acschembio.7b00903, PMID 29202222.

[10] Burz, C.; Aziz, B. Y.; Bălăcescu, L.; Leluţiu, L.; Buiga, R.; Samasca, G.; Irimie, A.; Lisencu, C., Tumor markers used in monitoring the tumor recurrence in patients with colorectal cancer. *Clujul. Med.,* **2016**, *89* (3), 378-83. DOI: 10.15386/cjmed-635, PMID 27547057.

[11] Tomuleasa, C.; Braicu, C.; Irimie, A.; Craciun, L.; Berindan-Neagoe, I., Nanopharmacology in translational hematology and oncology. *Int. J. Nanomedicine*., **2014**, *9*, 3465-79. DOI: 10.2147/IJN.S60488, PMID 25092977.

[12] Braicu, C.; Buse, M.; Busuioc, C.; Drula, R.; Gulei, D.; Raduly, L.; Rusu, A.; Irimie, A.; Atanasov, A. G.; Slaby, O.; Ionescu, C.; Berindan-Neagoe, I., A comprehensivereview on MAPK: Apromisingtherapeutictarget in cancer. *Cancer*., **2019**, *11* (10), 1618. DOI: 10.3390/cancers11101618, PMID 31652660.

[13] Olivero-Acosta, M.; Maldonado-Rojas, W.; Olivero-Verbel, J., Natural products as chemopreventiveagents by potentialinhibition of the kinasedomain in ErbB receptors. *Molecules*., **2017**, *22* (2), 308. DOI: 10.3390/molecules22020308, PMID 28218686.

[14] Songtawee, N.; Bevan, D. R.; Choowongkomon, K., Molecular dynamics of the asymmetric dimers of EGFR: simulations on the active and inactive conformations of the kinase domain. *J. Mol. Graph. Model*., **2015**, *58*, 16-29. DOI: 10.1016/j.jmgm.2015.03.002, PMID 25805329.

[15] Shan, Y.; Eastwood, M. P.; Zhang, X.; Kim, E. T.; Arkhipov, A.; Dror, R. O.; Jumper, J.; Kuriyan, J.; Shaw, D. E., Oncogenic mutations counteract intrinsic disorder in the EGFR kinase and promote receptor dimerization. Cell **2012**, *149* (4), 860-70. DOI: 10.1016/j.cell.2012.02.063, PMID 22579287.

[16] Park, E.; Kim, N.; Ficarro, S. B.; Zhang, Y.; Lee, B. I.; Cho, A.; Kim, K.; Park, A. K. J.; Park, W. Y.; Murray, B.; Meyerson, M.; Beroukhim, R.; Marto, J. A.; Cho, J.; Eck, M. J., Structure and mechanism of activity-based inhibition of the EGF receptor by Mig6. *Nat. Struct. Mol. Biol.,* **2015**, *22* (9), 703-11. DOI: 10.1038/nsmb.3074, PMID 26280531.

[17] Roskoski, R. Jr., ErbB/HER protein-tyrosine kinases: structures and small molecule inhibitors. *Pharmacol. Res.,* **2014**, *87*, 42-59. DOI: 10.1016/j.phrs.2014.06.001, PMID 24928736.

[18] Xie, Y. H.; Chen, Y. X.; Fang, J. Y., Comprehensive review of targeted therapy for colorectal cancer. *Signal Transduct. Target Ther.,* **2020**, *5* (1), 22. DOI: 10.1038/s41392-020-0116-z, PMID 32296018.

[19] Septelia, I. W.; Agus, L.; Elvira, Y.; Resda, A. S.; Melva, L.; Agung, E. W., Sekar, A., *In silico* and in vitro studies

on the anti-cancer activity of andrographolide targeting survivin in human breast cancer stem cells. *PLoS One.,* **2020**, *15* (11), e0240020.doi: 10.1371/journal.pone.0240020.

[20] Red, B. M.; Yun, C. H.; Lai, D.; Lemmon, M. A.; Eck, M. J.; Pao, W., Mechanism for activation of mutated epidermal growth factor receptors in lung cancer. *Proc.Natl.Acad. Sci. USA*., **2013**, *110* (38), E3595-604. DOI: 10.1073/pnas.1220050110, PMID 24019492.

[21] Sutto, L.; Gervasio, F. L., Effects of oncogenic mutations on the conformational free-energy landscape of EGFR kinase. *Proc. Natl. Acad. Sci. USA*., **2013**, *110* (26), 10616-21. DOI: 10.1073/pnas.1221953110, PMID 23754386.

[22] Jänne, P. A.; Yang, J. C.; Kim, D. W; Planchard, D.; Ohe, Y.; Ramalingam, S. S.; Ahn, M. J.; Kim, S. W; Su, W. C.; Horn, L.; Haggstrom. D.; Felip, E.; Kim, J. H.; Frewer, P.; Cantarini, M.; Brown, K. H.; Dickinson, P.A.; Ghiorghiu, S.; Ranson, M., AZD9291 in EGFR inhibitor-resistant non-small-cell lung cancer. *N. Engl. J. Med.*, **2015**, *372* (18), 1689-99. DOI: 10.1056/NEJMoa1411817, PMID 25923549.

[23] Breen, M. E.; Soellner, M. B., Small molecule substrate phosphorylation site inhibitors of protein kinases: approaches and challenges. *ACS. Chem. Biol*., **2015**, *10* (1), 175-89. DOI: 10.1021/cb5008376, PMID 25494294.

[24] Sordella, R.; Bell, D. W.; Haber, D. A.; Settleman, J., Gefitinib-sensitizing EGFR mutations in lung cancer activate anti-apoptotic pathways. *Science*., **2004**, *305* (5687), 1163-7. DOI: 10.1126/science.1101637, PMID 15284455.

[25] Merlo, V.; Longo, M.; Novello, S.; Scagliotti, G. V., EGFR pathway in advanced non-small cell lung cancer. *Front. Biosci. (Schol Ed)*., **2011**, *3*, 501-17. DOI: 10.2741/s168, PMID 21196393.

[26] Van den Eynde, M.; Baurain, J. F.; Mazzeo, F.; Machiels, J. P., Epidermal growth factor receptor targeted therapies for solid tumours. *Acta.Clin. Belg.,* **2011**, *66* (1), 10-7. DOI: 10.2143/ACB.66.1.2062508, PMID 21485758.

[27] Sherman, S. I., Targeted therapies for thyroid tumors. *Mod. Pathol.,* **2011**, *24* (Suppl 2), S44-52. DOI: 10.1038/modpathol.2010.165, PMID 21455200.

[28] Medina, P. J.; Goodin, S., Lapatinib: a dual inhibitor of human epidermal growth factor receptor tyrosine kinases. *Clin. Ther.,* **2008**, *30* (8), 1426-47. DOI: 10.1016/j.clinthera.2008.08.008, PMID 18803986.

[29]Johnston, S. R.; Leary, A., Lapatinib: a novel EGFR/HER2 tyrosine kinase inhibitor for cancer. *Drugs Today (Barc).,* **2006**, *42* (7), 441-53. DOI: 10.1358/dot.2006.42.7.985637, PMID 16894399.

[30] Forsythe, B.; Faulkner, K., Overview of the tolerability of gefitinib (IRESSA) monotherapy: clinical experience in non-small-cell lung cancer. *Drug. Saf*., **2004**, *27* (14), 1081-92. DOI: 10.2165/00002018-200427140-00002, PMID 15554744.

[31] Kumar, J. A.; Divya, J., Traditional and Ethnobotanical uses Premna barbata Wall. Ex Schauer in Kumaun and Garhwal Regions of Uttarakhand, India and Other Western Himalayan Countries- A Review. *Phyto*., **2017**, *9* (9), 1213-16. DOI: 10.25258/phyto.v9i09.10308.

[32]Tamta, M.; Kumar, A.; Shukla, N.; Negi, D., Effects of crude extracts of Premna barbata Wall. and Clerodendrum viscosum Vent. (Verbenaceae) on different pathogenic bacteria. *Asian. J. Tradit. Med.,* **2012**, *7* (1), 1-7.http://asianjtm.syphu.edu.cn/EN/Y2012/V7/I1/1

[33] Negi, S.; Shukla, V.; Rawat, M. S. M.; Pant, G.; Nagatsu, A., Premnosidic acid, a new iridoid glycoside from Premma barbata. Cheminform., **2004**, *35*, 1805-6. DOI: 10.1002/chin.200450151

[34] Yadav, D.; Masood, N.; Luqman, S.; Brindha, P.; Gupta, M. M., Antioxidant furofuran lignans from Premna integrifolia. *Ind. Crops. Prod.,* **2013**, *41*, 397-402. DOI: 10.1016/j.indcrop.2012.04.044.

[35] Rao, C. B.; Vijayakumar, E. K.; Vijayalakshmi, K. V., Iridoids from Premna latifolia. *Planta. Med.,* **1981**, *41* (1), 80-3. DOI: 10.1055/s-2007-971680, PMID 17401822.

[36] Ghisalberti, E. L., Biological and pharmacological activity of naturally occurring iridoids and secoiridoids. *Phytomed.,* **1998**, *5* (2), 147-63. DOI: 10.1016/S0944-7113(98)80012-3, PMID 23195768.

[37] Stamos, J.; Sliwkowski, M. X.; Eigenbrot, C., Structure of the epidermal growth factor receptor kinase domain alone and in complex with a 4-anilinoquinazoline

inhibitor. *J. Biol. Chem.,* **2002**, *277* (48), 46265-72. DOI: 10.1074/jbc.M207135200, PMID 12196540.

[38] Hsu, H. Y.; Yang, J. J.; Lin, S. Y.; Lin, C. C., Comparisons of geniposidic acid and geniposide on antitumor and radioprotection after sublethal irradiation. *Cancer. Lett.,* **1997**, *113* (1-2), 31-7. DOI: 10.1016/s0304-3835(96)04572-7.

[39] Weisberg, E.; Manley, P. W.; Breitenstein, W.; Brüggen, J.; Cowan-Jacob, S. W.; Ray, A.; Huntly, B.; Fabbro, D.; Fendrich, G.; Hall-Meyers, E.; Kung, A. L.; Mestan, J.; Daley, G. Q.; Callahan, L.; Catley, L.; Cavazza, C.; Azam, M.; Neuberg, D.; Wright, R. D.; Gilliland, D. G.; Griffin, J. D., Characterization of AMN107, a selective inhibitor of native and mutant bcr-abl. *Cancer. Cell.*, **2005**, *7* (2), 129-41. DOI: 10.1016/j.ccr.2005.01.007, PMID 15710326.

[40] Shiau, A. K.; Barstad, D.; Loria, P. M.; Cheng, L.; Kushner, P. J.; Agard, D. A.; Greene, G. L., The structural basis of estrogen receptor/coactivator recognition and the antagonism of this interaction by tamoxifen. Cell., **1998**, *95* (7), 927-37. DOI: 10.1016/s0092-8674(00)81717-1, PMID 9875847.

[41] M.; Kuhtinskaja, O.; Bragina, M.; Kulp, M., Vaher, Anticancer Effect of the Iridoid Glycoside Fraction from Dipsacus fullonum L. Leaves. *Natural, Product. Communications.,* **2020**, *15* (9), 1-6. DOI: 10.1177/1934578X20951417.

[42] Petit-Topin, I.; Fay, M.; Resche-Rigon, M.; Ulmann, A.; Gainer, E.; Rafestin-Oblin, M. E.; Fagart, J., Molecular determinants of the recognition of ulipristal acetate by oxo-steroid receptors. *J. Steroid. Biochem. Mol. Biol.,* **2014**, *144* (B), 427-35. DOI: 10.1016/ j.jsbmb.2014.08.008, PMID 25204619.

[43] Ramamurthy, V.; Krystek, S. R.; Bush, A.; Wei, A.; Emanuel, S. L.; Dasgupta, R.; Janjua, A.; Cheng, L.; Murdock, M.; Abramczyk, B.; Cohen, D.; Lin, Z.; Morin, P.; Davis, J. H.; Dabritz, M.; McLaughlin, D. C.; Russo, K. A.; Chao, G.; Wright, M. C.; Jenny, V. A.; Engle, L. J.; Furfine, E; Sheriff, S.; Bush, A., Structures of adnectin/protein complexes reveal an expanded binding footprint. *Structure.,* **2012**, *20* (2), 259-69. DOI: 10.1016/j.str.2011.11.016, PMID 22325775.

[44] Watt, W.; Koeplinger, K. A.; Mildner, A. M.; Heinrikson, R. L.; Tomasselli, A. G.; Watenpaugh, K. D., The atomic-resolution structure of human caspase-8, a key activator of apoptosis. *Structure.,* **1999**, *7* (9), 1135-43. DOI: 10.1016/s0969-2126(99)80180-4, PMID 10508785.

[45] Aertgeerts, K.; Skene, R.; Yano, J.; Sang, B. C.; Zou, H.; Snell, G.; Jennings, A.; Iwamoto, K.; Habuka, N.; Hirokawa, A.; Ishikawa, T.; Tanaka, T.; Miki, H.; Ohta, Y.; Sogabe, S., Structural analysis of the mechanism of inhibition and allosteric activation of the kinase domain of HER2 protein. *J. Biol. Chem.,* **2011**, *286* (21), 18756-65. DOI: 10.1074/jbc.M110.206193, PMID 21454582.

[46] McTigue, M.; Murray, B. W.; Chen, J. H.; Deng, Y. L.; Solowiej, J.; Kania, R. S., Molecular conformations, interactions, and properties associated with drug efficiency and clinical performance among VEGFRTK inhibitors. *Proc. Natl. Acad. Sci. USA.,* **2012**, *109* (45), 18281-9. DOI: 10.1073/pnas.1207759109, PMID 22988103.

[47] Park, J. H.; Liu, Y.; Lemmon, M. A.; Radhakrishnan, R., Erlotinib binds both inactive and active conformations of the EGFR tyrosine kinase domain. *Biochem. J.,* **2012**, *448* (3), 417-23. DOI: 10.1042/BJ20121513, PMID 23101586.

[48] Hasegawa, M.; Nishigaki, N.; Washio, Y.; Kano, K.; Harris, P. A.; Sato, H.; Mori, I.; West, R. I.; Shibahara, M.; Toyoda, H.; Wang, L.; Nolte, R. T.; Veal, J. M.; Cheung, M., Discovery of novel benzimidazoles as potent inhibitors of TIE-2 and VEGFR-2 tyrosine kinase receptors. *J. Med. Chem.,* **2007**, *50* (18), 4453-70. DOI: 10.1021/jm0611051, PMID 17676829.

[49] Fischmann, T. O.; Smith, C. K.; Mayhood, T. W.; Myers, J. E.; Reichert, P.; Mannarino, A.; Carr, D.; Zhu, H.; Wong, J.; Yang, R. S.; Le, H. V.; Madison, V. S., Crystal structures of MEK1 binary and ternary complexes with nucleotides and inhibitors. *Biochemistry.,* **2009**, *48* (12), 2661-74. DOI: 10.1021/bi801898e, PMID 19161339.

[50] Hatzivassiliou, G.; Haling, J. R.; Chen, H.; Song, K.; Price, S.; Heald, R.; Hewitt, J. F.; Zak, M.; Peck, A.; Orr, C.; Merchant, M.; Hoeflich, K. P.; Chan, J.; Luoh, S.M., Anderson, D. J.; Ludlam, M. J.; Wiesmann, C.; Ultsch, M.; Friedman, L. S.; Malek, S.; Belvin, M., Mechanism of MEK inhibition determines efficacy in mutant KRAS-*versus* BRAF-driven cancers. *Nature.,* **2013**, *501* (7466), 232-6. DOI: 10.1038/nature12441, PMID

23934108.

[51] Red, B. M.; Choi, S. H.; Alvarado, D.; Moravcevic, K.; Pozzi, A.; Lemmon, M. A.; Carpenter, G., The juxtamembrane region of the EGF receptor functions as an activation domain. *Mol. Cell.,* **2009**, *34* (6), 641-51. DOI: 10.1016/j.molcel.2009.04.034, PMID 19560417.

[52] Yasuda, H.; Park, E.; Yun, C. H.; Sng, N. J.; Lucena-Araujo, A. R.; Yeo, W. L.; Huberman, M. S.; Cohen, D. W.; Nakayama, S.; Ishioka, K.; Yamaguchi, N.; Hanna, M.; Oxnard, G. R.; Lathan, C. S.; Moran, T.; Sequist, L. V.; Chaft, J. E.; Riely, G. J.; Arcila, M. E.; Soo, R. A.; Meyerson, M.; Eck, M. J.; Kobayashi, S. S.; Costa, D. B., Structural, biochemical, and clinical characterization of epidermal growth factor receptor (EGFR)exon 20 insertion mutations in lung cancer. *Sci. Transl. Med.,* **2013**, *5* (216), 216ra177. DOI: 10.1126/scitranslmed.3007205, PMID 24353160.

[53] Park, E., Kim, N.; Ficarro, S. B., Zhang, Y.; Lee, B. I.; Cho, A.; Kim, K.; Park, A. K. J.; Park, W. Y.; Murray, B.; Meyerson, M.; Beroukhim, R.; Marto, J. A.; Cho, J.; Eck, M. J., Structure and mechanism of activity-based inhibition of the EGF receptor by Mig6. *Nat. Struct. Mol. Biol.,* **2015**, *22* (9), 703-11. DOI: 10.1038/nsmb.3074, PMID 26280531.

[54] Matsuda, T.; Ito, T.; Takemoto, C.; Katsura, K.; Ikeda, M.; Wakiyama, M.; Kukimoto-Niino, M.; Yokoyama, S.; Kurosawa, Y.; Shirouzu, M., Cell-free synthesis of functional antibody fragments to provide a structural basis for antibody-antigen interaction. *PLOSONE.*, **2018**, *13* (2), e0193158. DOI: 10.1371/journal.pone.0193158, PMID 29462206.

[55] Littler, D. R.; Alvarez-Fernández, M.; Stein, A.; Hibbert, R. G.; Heidebrecht, T.; Aloy, P.; Medema, R. H.; Perrakis, A., Structure of the FoxM1DNA-recognition domain bound to a promoter sequence. *Nucleic. Acids. Res.,* **2010**, *38* (13), 4527-38. DOI: 10.1093/nar/gkq194, PMID 20360045.

[56] Trott, O.; Olson, A. J., AutoDock Vina: improving the speed and accuracy of docking with a new scoring function, efficient optimization, and multithreading. *J. Comput. Chem.,* **2010**, *31* (2), 455-61. DOI: 10.1002/jcc.21334, PMID 19499576.

[57] O'Boyle, N. M.; Banck, M.; James, C. A.; Morley, C.; Vandermeersch, T.; Hutchison, G. R., Open Babel: an open chemical toolbox. *J. Cheminform.,* **2011**, *3*, 33. DOI: 10.1186/1758-2946-3-33, PMID 21982300.

[58] Waterhouse, A.; Bertoni, M.; Bienert, S.; Studer, G.; Tauriello, G.; Gumienny, R.; Heer, F. T.; de Beer, T. A. P.; Rempfer, C.; Bordoli, L.; Lepore, R.; Schwede, T., SWISS-MODEL: homology modelling of protein structures and complexes. *Nucleic. Acids. Res.*, **2018**, *46* (W1), W296-303. DOI: 10.1093/nar/gky427, PMID 29788355.

[59] Banerjee, P.; Dunkel, M.; Kemmler, E.; Preissner, R., SuperCYPsPred-a web server for the prediction of cytochrome activity. *Nucleic. Acids. Res.,* **2020**, *48* (W1), W580-5. DOI: 10.1093/nar/gkaa166, PMID 32182358.

[60] Saha, S.; Pal, D.; Nimse, S. B., Recent Advances in the Discoveryof GSK-3 Inhibitors from Synthetic Origin in the Treatment of Neurological Disorders. *Current. Drug. Target.,* **2021**, *22* (12), 1437-61. DOI: 10.2174/1389450122666210120143953.

[61] El-Rayes, B. F.; LoRusso, P. M., Targeting the epidermal growth factor receptor. *Br. J. Cancer.,* **2004**, *91* (3), 418-24. DOI: 10.1038/sj.bjc.6601921, PMID 15238978.

[62] Jiang, W.; Ji, M., Receptor tyrosine kinases in PI3K signaling: the therapeutic targets in cancer. *Semin. Cancer. Biol.,* **2019**, *59*, 3-22. DOI: 10.1016/j.semcancer.2019.03.006, PMID 30943434.

[63] Cuenda, A.; Lizcano, J. M.; Lozano, J., Editorial: mitogen activated protein kinases. *Front. Cell. Dev. Biol.,* **2017**, *5*, 80. DOI: 10.3389/fcell.2017.00080, PMID 28959688.

[64] Padrao, N. A.; Mayayo-Peralta, I. M.; Zwart, W., Targeting mutated estrogen receptor alpha: rediscovering old and identifying new therapeutic strategies in metastatic breast cancer treatment. *Curr. Opin. Endocr. Metab. Res.,* **2020**, *15*, 43-8. DOI: 10.1016/j.coemr.2020.10.008.

[65] Bergantin, L. B., Diabetes and cancer: debating the link through Ca^{2+}/cAMP signalling. *Cancer. Lett.,* **2019**, *448:*128-31. DOI: 10.1016/j.canlet.2019.02.017, PMID 30771427.

[66] Chuang, H. H.; Zhen, Y. Y.; Tsai, Y. C.; Chuang, C.H.; Huang, M. S.; Hsiao, M.; Yang, C. J., Targeting Pin1 for modulation of cellmotility and cancertherapy.

Biomedicine., **2021**, *9* (4), 359. DOI: 10.3390/ biomedicines9040359, PMID 33807199.

[67] Yao, S.; Fan, L. Y.; Lam, E. W., The FOXO3-FOXM1 axis: A key cancer drug target and a modulator of cancer drug resistance. *Semin. Cancer. Biol.,* **2018**, *50*, 77-89. DOI: 10.1016/j.semcancer.2017.11.018, PMID 29180117.

[68] Yadav, P.; Yadav, R.; Jain, S.; Vaidya, A., Caspase-3: A primary target for natural and synthetic compounds for cancer therapy. *Chem. Biol. Drug. Des.,* **2021**, *98* (1), 144-65. DOI: 10.1111/cbdd.13860, PMID 33963665.

[69] Schlam, I.; Swain, S. M., HER2-positive breast cancer and tyrosine kinase inhibitors: the time is now. npj*Breast. Cancer.,* **2021**, *7* (1), 56. DOI: 10.1038/s41523-021-00265-1, PMID 34016991.

[70] Amani, J.; Gorjizadeh, N.; Younesi, S.; Najafi, M.; Ashrafi, A. M.; Irian, S.; Gorjizadeh, N.; Azizian, K., Cyclin-dependent kinase inhibitors (CDKIs) and the DNA damage response: the link between signaling pathways and cancer. *DNA. Repair.,* **2021**, *102*, 103103. DOI: 10.1016/j.dnarep.2021.103103.

[71] Gundala, R.; Balutia, H.; Lavanya, R.; Velayutham, R.; Roy, K. K., HCV NS3 serine protease as a drug target for the development of drugs against hepatocellular carcinoma (liver cancer). In: Cancer-leadingproteases. *Academic. Press.,* **2020**, 243-63. DOI: 10.1016/B978-0-12-818168-3.00009-7.

[72] Abdel-Rahman, O., Targeting vascular endothelial growth factor (VEGF) pathway in gastric cancer: preclinical and clinical aspects. *Crit. Rev. Oncol. Hematol.,* **2015**, *93* (1), 18-27. DOI: 10.1016/ j.critrevonc.2014.05.012, PMID 24970311.

[73] Bradbury, J., Rapamycin: a future in cancer treatment? *Lancet. Oncol.,* **2002**, *3* (3), 131. DOI: 10.1016/S1470-2045(02)00668-X.

[74] Ekizceli, G.; Uluer, E. T.; Inan, S., Investigation of the effects of rapamycin on the mTOR pathway and apoptosis in metastatic and non-metastatic human breast cancer cell lines. *Bratisl. Lek. Listy.,* **2020**, *121* (4), 308-15. DOI: 10.4149/BLL_2020_049, PMID 32356448.

[75] Shi, J. Y.; Huang, Z. R.; Gao, H. Y.; Xu, X. L., Anticancer effects of juglone in OVCAR-3 human ovarian carcinoma are facilitated through programmed cell death, endogenous ROS production, inhibition of cell migration and invasion and cell cycle arrest. *J. Buon.,* **2020**, *25* (2), 779-84. PMID 32521867.

[76] Wang, X. J.; Etzkorn, F. A., Peptidyl-prolyl isomerase inhibitors. *Biopolymer.,* **2006**, *84* (2), 125-46. DOI: 10.1002/bip.20240, PMID 16302169.

[77] Dubiella, C.; Pinch, B. J.; Koikawa, K.; Zaidman, D.; Poon, E.; Manz, T. D.; Nabet, B.; He, S.; Resnick, E.; Rogel, A.; Langer, E. M.; Daniel, C. J.; Seo, H. S.; Chen, Y.; Adelmant, G.; Sharifzadeh, S.; Ficarro, S. B.; Jamin, Y.; Martins. da Costa. B.; Zimmerman, M. W.; Lian, X.; Kibe, S.; Kozono, S.; Doctor, Z. M.; Browne, C. M.; Yang, A.; Stoler-Barak, L.; Shah, R. B.; Vangos, N. E.; Geffken, E. A.; Oren, R.; Koide, E.; Sidi, S.; Shulman, Z.; Wang, C.; Marto, J. A.; Dhe-Paganon, S.; Look, T.; Zhou, X. Z.; Lu, K. P.; Sears, R. C.; Chesler, L.; Gray, N. S.;, London, N., Sulfopin is a covalent inhibitor of Pin1 that blocks Myc-driven tumors *in vivo*. *Nat. Chem. Biol.,* **2021**, *17:* 954-63. DOI: 10.1038/s41589-021-00786-7, PMID 33972797.

[78] Quarato, G.; D'Aprile, A.; Gavillet, B.; Vuagniaux, G.; Moradpour, D.; Capitanio, N.; Piccoli, C., The cyclophilin inhibitor alisporivir prevents hepatitis C virus-mediated mitochondrial dysfunction. *Hepatology.,* **2012**, *55* (5), 1333-43. DOI: 10.1002/ hep.25514, PMID 22135208.

[79] Zhang, X.; Fang, X.; Gao, Z.; Chen, W.; Tao, F.; Cai, P.; Yuan, H.; Shu, Y.; Xu, Q.; Sun, Y.; Gu, Y., Axitinib, a selective inhibitor of vascular endothelial growth factor receptor, exerts an anticancer effect in melanoma through promoting antitumor immunity. *Anticancer. Drugs.,* **2014**, *25* (2), 204-11. DOI: 10.1097/ CAD.0000000000000033, PMID 24135499.

[80] Kelly, R. J.; Rixe, O., Axitinib-a selective inhibitor of the vascular endothelial growth factor (VEGF) receptor. *Target. Oncol.,* **2009**, *4* (4), 297-305. DOI: 10.1007/s11523-009-0126-9, PMID 19876699.

[81] Ueda, K.; Suekane, S.; Hirano, T.; Ogasawara, N.; Chikui, K.; Uemura, K.; Nakiri, M.; Nishihara, K.; Matsuo, M.; Igawa, T., Efficacy of axitinib as second-line treatment in locallyadvanced and metastaticrenalcellcarcinoma. *Anticancer. Res.,* **2018**, *38* (9), 5387-92. DOI: 10.21873/anticanres.12868, PMID 30194193.

[82] Sanphui, P.; Rajput, L.; Gopi, S. P.; Desiraju, G. R., New multi-component solid forms of anti-cancer drug erlotinib: role of auxiliary interactions in determining a preferred conformation. *Acta. Crystallogr. B. Struct. Sci. Cryst. Eng. Mater.,* **2016**, *72* (3), 291-300. DOI: 10.1107/S2052520616003607, PMID 27240760.

[83] Saha, S.; Yeom, G. S.; Nimse, S. B.; Pal, D., Combination Therapy of Ledipasvir and Itraconazole in the Treatment of COVID-19 Patients Coinfected with Black Fungus: An *In Silico* Statement. *Biomed. Res. Int.,* **2022**, Article ID 5904261. https://doi.org/10.1155/2022/5904261.

[84] Zinad, D. S.; Mahal, A.; Salman, G. A.; Shareef, O. A.; Pratama, M. R. F., Molecular Docking and DFT Study of Synthesized Oxazine Derivatives. *Egypt. J. Chem.,* **2022**, *65*, 231-40. DOI: 10.21608/ ejchem.2021.102664.4755.

[85] Jin, R. Y.; Zeng, C. Y.; Liang, X. H.; Sun, X. H.; Liu, Y. F.; Wang, Y. Y.; Zhou, S., Design, synthesis, biological activities and DFT calculation of novel 1,2,4-triazole Schiff base derivatives. *Bioorg. Chem.,* **2018**, *80*, 253-60.https://doi.org/10.1016/j.bioorg.2018.06.030.